AD_____

Award Number: DAMD17-02-1-0506

TITLE: Nanoparticle-Mediated p53 Gene Therapy for Breast Cancer

PRINCIPAL INVESTIGATOR: Swayam Prabha
Vinod D. Labhasetwar

CONTRACTING ORGANIZATION: University of Nebraska Medical Center
Omaha, NE 69198-7835

REPORT DATE: April 2004

TYPE OF REPORT: Annual Summary

PREPARED FOR: U.S. Army Medical Research and Materiel Command
Fort Detrick, Maryland 21702-5012

DISTRIBUTION STATEMENT: Approved for Public Release;
Distribution Unlimited

The views, opinions and/or findings contained in this report are
those of the author(s) and should not be construed as an official
Department of the Army position, policy or decision unless so
designated by other documentation.

REPORT DOCUMENTATION PAGE

Form Approved
OMB No. 074-0188

1. AGENCY USE ONLY (Leave blank)	2. REPORT DATE April 2004	3. REPORT TYPE AND DATES COVERED Annual Summary (15 Mar 2003 - 14 Mar 2004)

4. TITLE AND SUBTITLE

Nanoparticle-Mediated p53 Gene Therapy for Breast Cancer

5. FUNDING NUMBERS

DAMD17-02-1-0506

6. AUTHOR(S)
Swayam Prabha
Vinod D. Labhasetwar

7. PERFORMING ORGANIZATION NAME(S) AND ADDRESS(ES)
University of Nebraska Medical Center
Omaha, NE 69198-7835

E-Mail: sprabha@unmc.edu

8. PERFORMING ORGANIZATION REPORT NUMBER

9. SPONSORING / MONITORING AGENCY NAME(S) AND ADDRESS(ES)

U.S. Army Medical Research and Materiel Command
Fort Detrick, Maryland 21702-5012

10. SPONSORING / MONITORING AGENCY REPORT NUMBER

11. SUPPLEMENTARY NOTES

Original contains color plates. All DTIC reproductions will be in black and white.

12a. DISTRIBUTION / AVAILABILITY STATEMENT
Approved for Public Release; Distribution Unlimited

12b. DISTRIBUTION CODE

13. ABSTRACT (Maximum 200 Words)

Gene expression with non-viral vectors is usually transient and lasts only for few days. Therefore, repeated injection of the expression vector is required to maintain a therapeutic protein concentration in the target tissue. Biodegradable nanoparticles (~ 200 nm diameter) formulated using biocompatible polymer, poly(D,L-lactide-*co*-glycolide) (PLGA) have the potential for sustained gene delivery. Our hypothesis is that the nanoparticle-mediated gene delivery would result in sustained gene expression, and hence better efficacy with a therapeutic gene. Nanoparticles loaded with *wt*-p53 DNA demonstrated greater and sustained antiproliperative activity *in vitro* as compared to that with naked DNA and DNA-liposome complex. The greater efficacy of *wt*-p53 DNA-loaded nanoparticles was attributed to sustained intracellular DNA delivery and gene expression. A single-dose intratumoral administration of *wt*-p53 DNA-loaded nanoparticles demonstrated significant inhibition of tumor growth in MDAMB-435-induced subcutaneous breast cancer mouse model that also resulted in prolonged animal survival than controls. The mechanism of inhibition of tumor growth with *wt*-p53-DNA-loaded nanoparticles was attributed to higher apoptosis of tumor cells than that in controls, and also the induction of antiangiogenic protein, thrombospondin-I that inhibited tumor angiogenesis. The studies thus demonstrate the efficacy of nanoparticles as a non-viral gene expression vector and their potential application in breast cancer therapy.

14. SUBJECT TERMS
Sustained local gene delivery, Apoptosis, Nanoparticles, p53, Polymer, Non-viral gene delivery systems

15. NUMBER OF PAGES
33

16. PRICE CODE

17. SECURITY CLASSIFICATION OF REPORT Unclassified	18. SECURITY CLASSIFICATION OF THIS PAGE Unclassified	19. SECURITY CLASSIFICATION OF ABSTRACT Unclassified	20. LIMITATION OF ABSTRACT Unlimited

NSN 7540-01-280-5500

Standard Form 298 (Rev. 2-89)
Prescribed by ANSI Std. Z39-18
298-102

Table of Contents

INTRODUCTION

p53, a tumor suppressor gene, encodes a nuclear phosphoprotein involved in the control of cell growth and apoptosis. Breast cancer is associated with a high degree of mutations in the p53 gene that leads to loss of apoptotic control over cell proliferation. Transfection of tumor cells with p53 gene would result in the restoration of normal p53 protein functions in the cell. The purpose of this project is to investigate nanoparticles, a colloidal polymeric gene delivery system of ~100 nanometer diameter, formulated from a FDA-approved, biodegradable and biocompatible polymer, poly(DL-lactide-co-glycolide) (PLGA), for the treatment of breast cancer. Four specific aims proposed are as follows:

1. To formulate and characterize p53 gene-containing nanoparticles.
2. To study the mechanism of gene transfer using nanoparticles.
3. To study the sustained inhibition of proliferation of human breast cancer cells with p53 gene-loaded nanoparticles.
4. To study the efficacy of nanoparticle mediated p53 gene therapy in effecting a long-term tumor inhibition and regression in a mouse model of breast cancer.

This report summarizes the finding from the specific aim 3 and 4 and is outlined based on the statement of work.

Task 2: Cell culture studies

1. To study the sustained inhibition of proliferation of human breast cancer cells (MDAMB-435S) with nanoparticles using a standard cell proliferation assay, months 12-15.

We determined the antiproliferative activity of wt-p53 gene-loaded nanoparticles in breast cancer cell line. Nanoparticles containing plasmid DNA were formulated using a multiple-emulsion-solvent evaporation technique, and the antiproliferative activity of the gene-loaded nanoparticles was determined in MDA-MB435S cells. To understand the mechanism of sustained gene expression with nanoparticles, we monitored the intracellular localization of TOTO-labeled DNA and also determined p53 mRNA levels over a period of time. Nanoparticles demonstrated sustained and significantly greater inhibition of cell proliferation than naked DNA alone (Fig 1) or DNA complexed with commercially available transfecting agent (Lipofectamine™) (Fig 2). Cells transfected with nanoparticles demonstrated sustained p53 mRNA levels compared to those transfected with plasmid DNA or liposome-DNA complex (Fig 3), thus explaining the sustained antiproliferative activity with nanoparticles. Studies with fluorescently-labeled DNA using confocal microscopy (Fig 4) and quantitative analyses using microplate reader (Fig 6) demonstrated sustained intracellular localization of DNA with nanoparticles, suggesting the slow release of DNA from nanoparticles localized inside the cells (up to 7 days). Cells transfected with plasmid DNA demonstrated only transient intracellular DNA levels (3 days). Colocalization of DNA with endo-lysosomes demonstrated that nanoparticles are capable of releasing DNA outside the endo-lysosomes when compared to naked DNA suggesting the potential of nanoparticles in releasing more DNA outside endo-lysosomes when compared to naked DNA (Fig 5). In conclusion, nanoparticle-mediated sustained wt-p53 gene delivery results in greater antiproliferative activity, which could be of therapeutic benefit in breast cancer treatment.

Task 3: In vivo studies, months 18 to 36

1. To study the efficacy of nanoparticle-mediated _in vivo_ wt-p53 gene transfer in effecting long-term tumor regression in a mouse model of breast cancer

Mice-bearing subcutaneous MDA-MB-435S human breast cancer xenografts were treated with a single-dose intra-tumoral injection of wt-p53-DNA loaded nanoparticles (dose equivalent to 50 μg DNA). Naked wt-p53 DNA, saline control and empty vector (p53-ve)-loaded nanoparticles were used as controls. Nanoparticles demonstrated significant and sustained tumor inhibition ($p < 0.05$) and better mice survival ($p < 0.05$) compared to naked DNA control that demonstrated only short-term inhibition of tumor following which rate of tumor growth was similar to that of saline and empty vector control (Fig 7). Also, nanoparticle-mediated p53 gene therapy resulted in better and significantly higher mice survival (Fig 8).
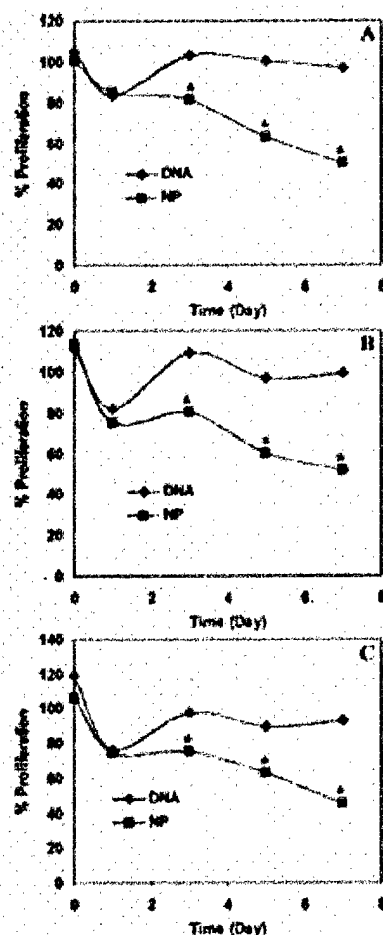
4

Figure 1. Antiproliferative activity of wt-p53 DNA-loaded nanoparticles (NP) and naked wt-p53 DNA (DNA) in MDAMB-435S cells. Cells (2500 cells/well) grown in 96-well plates were incubated with (A) 500, (B) 750, and (C) 1000 μg/mL nanoparticles and an equivalent amount of naked DNA [(A) 10.5, (B) 15.75, and (C) 21 μg/mL, respectively]. Medium control or nanoparticles without DNA were used as controls. Cell growth was followed using a standard MTS assay where the absorbance is directly proportional to the number of viable cells. Nanoparticles demonstrated an increase in antiproliferative activity with incubation time. Data are represented as the mean ± the standard error of the mean (n = 6; p < 0.01 for points marked with asterisks).
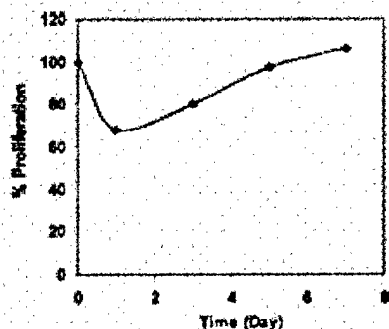

Figure 2. Antiproliferative activity of the wt-p53 DNA–Lipofectamine complex. MDAMB-435S cells (2500 cells/well) grown in 96-well plates were incubated with the DNA–Lipofectamine complex (DNA dose of 1.5 μg/mL), and cell proliferation was followed with a standard MTS assay. The DNA–Lipofectamine complex resulted in the transient inhibition of cell proliferation. Data are represented as the mean ± the standard error of the mean (n = 6).
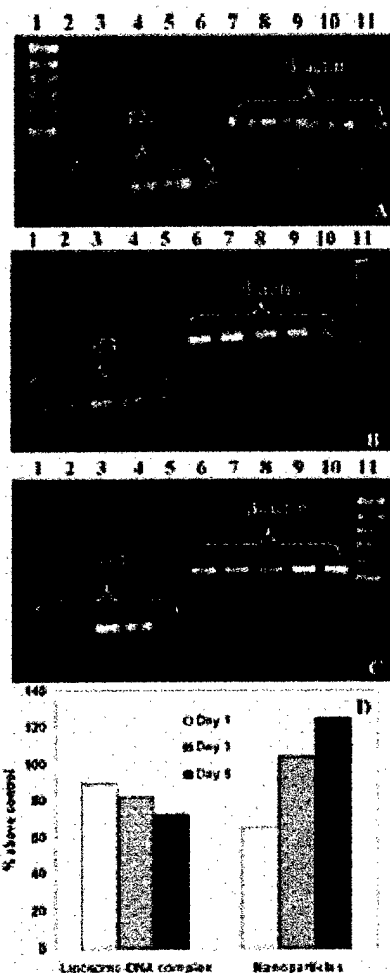
Figure 3. RT-PCR detection of p53 mRNA levels on day (A) 1, (B) 3, and (C) 5 on gel and quantitatively (D) using densitometry. (A) Lane 1: molecular weight markers. Lanes 2–6 (p53) and lanes 7–11 (β-actin): levels in cells transfected with wt-p53 DNA, p53(-ve) DNA-loaded nanoparticles, wt-p53 DNA-loaded nanoparticles, the wt-p53 DNA–Lipofectamine complex, and untreated cells, respectively. (B and C) Lane 11: molecular weight markers. Lanes 1–5 (p53) and lanes 6–10 (β-actin): levels in cells treated with wt-p53 DNA, p53-(-ve) DNA-loaded nanoparticles, wt-p53 DNA-loaded nanoparticles, the wt-p53 DNA–Lipofectamine complex, and untreated cells, respectively. Since untreated cells exhibited some basal levels of p53 mRNA, the quantitative data (D) are expressed as the percentage above the control. Cells transfected with wt-p53 DNA-loaded nanoparticles and the wt-p53 DNA–Lipofectamine complex exhibited detectable levels of p53 mRNA higher than baseline levels (untransfected cells). Cells transfected with wt-p53 DNA-loaded nanoparticles demonstrated sustained and increased p53 mRNA levels with incubation time as opposed to a decrease in mRNA levels in the cells transfected with the wt-p53 DNA–Lipofectamine complex.
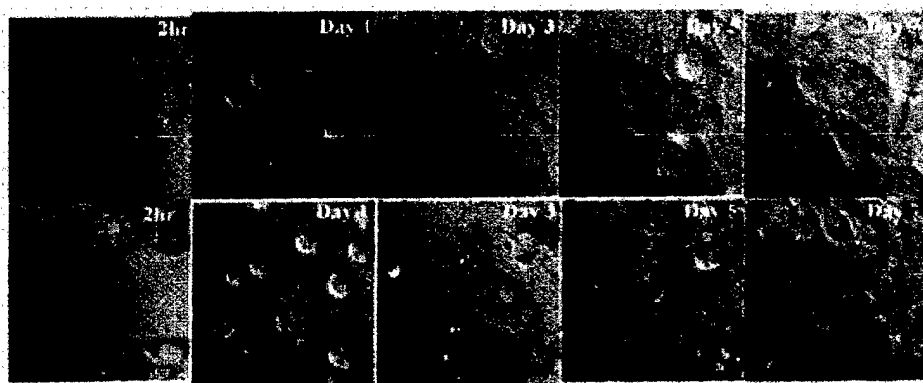
5

Figure 4. Time course study of intracellular uptake and retention of DNA in MDA-MB-435S cells. Cells were transfected with either naked DNA (red fluorescence, top panel) or nanoparticles (green fluorescence) loaded with DNA (red fluorescence, bottom panel). Cells transfected with nanoparticles demonstrated sustained intracellular DNA localization as opposed to transient localization in the cells transfected with naked DNA.
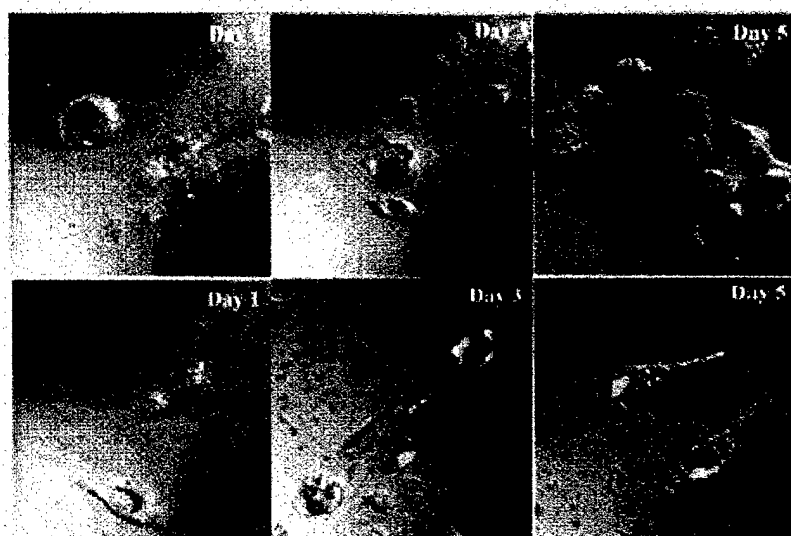

Figure 5. Time course study of the intracellular distribution of DNA. Cells transfected with naked YOYO-labeled DNA (top panel) or encapsulated in nanoparticles (bottom panel). Cells transfected with nanoparticles demonstrated a sustained and significantly greater amount of DNA localization in cytosol (green fluorescence) vs that in endolysosomes (yellow fluorescence due to colocalization of DNA LysoTracker Red, marker for endolysosomes). Cells transfected with naked DNA demonstrated a reduced level of green fluorescence after 3 days.
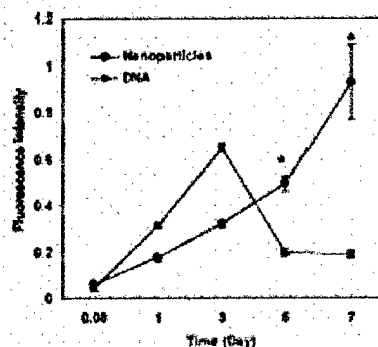

Figure 6. Quantitative determination of intracellular DNA levels. Cells transfected with YOYO-labeled DNA-loaded nanoparticles demonstrated sustained and increased intracellular DNA levels as opposed to transient DNA levels in the cells transfected with naked DNA. Data are represented as the mean $\pm$ the standard error of the mean ($n = 6$; $p < 0.001$ for points marked with asterisks).
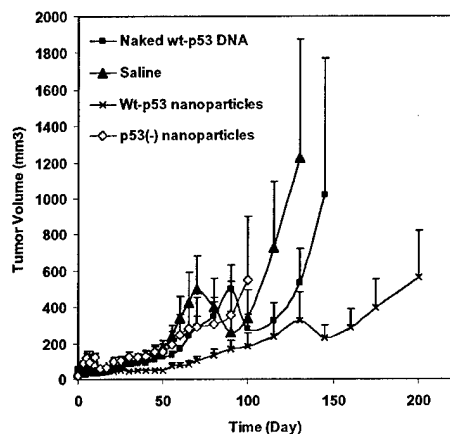
Figure 7. Effect of *wt*-p53-DNA-loaded nanoparticles on tumor volume in mice with breast tumor. Nanoparticles containing *wt*-p53 DNA (equivalent to 50 μg DNA) were injected intratumorally at day 0 and tumor volume was calculated as described in material and methods. Naked *wt*-p53 DNA, p53 (-ve) nanoparticles and saline-treated mice were used as controls. Results are expressed as mean ± SEM (n=8, * P<0.01 compared to naked DNA, saline control, and p53 (-ve) nanoparticles, # P<0.01, compared to saline control).

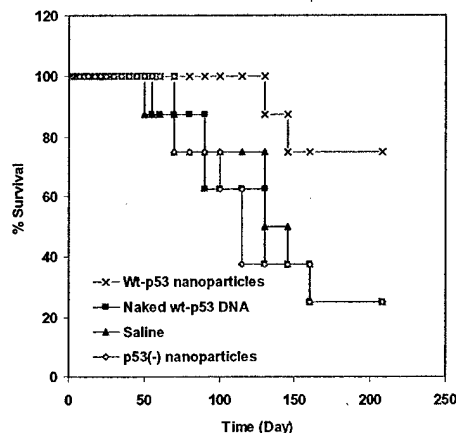**Figure 8.** Effect of *wt*-p53-DNA-loaded nanoparticles on survival rate of athymic nude mice in breast cancer model. *Wt*-p53-DNA-loaded nanoparticles-treated mice demonstrated better survival (log-rank statistics: χ^2 = 12.01, p = 0.0073) compared to *wt*-p53 naked DNA (p=0.0032), Saline (p=.0049) and p53 (-ve)-DNA-loaded nanoparticles (n=.0038).

2. To investigate the mechanism of tumor inhibition:

   The mechanism of p53-mediated tumor inhibition is complex and is mainly thought to be by two different pathways. While p53 transfection into cancerous cells induces apoptosis, both *in vitro* and *in vivo*, anti-angiogenic effect of p53 transfection on tumor endothelial cells is thought to play a significant role *in vivo* (*1*). It has also been established that p53 can induce both G1/S phase arrest and apoptosis in endothelial cells directly (*2*). Hence, in order to study the mechanism of nanoparticle-mediated tumor inhibition, thrombospondin (TSP-1) expression following p53 gene transfection was studied by immunohistochemistry and real time PCR
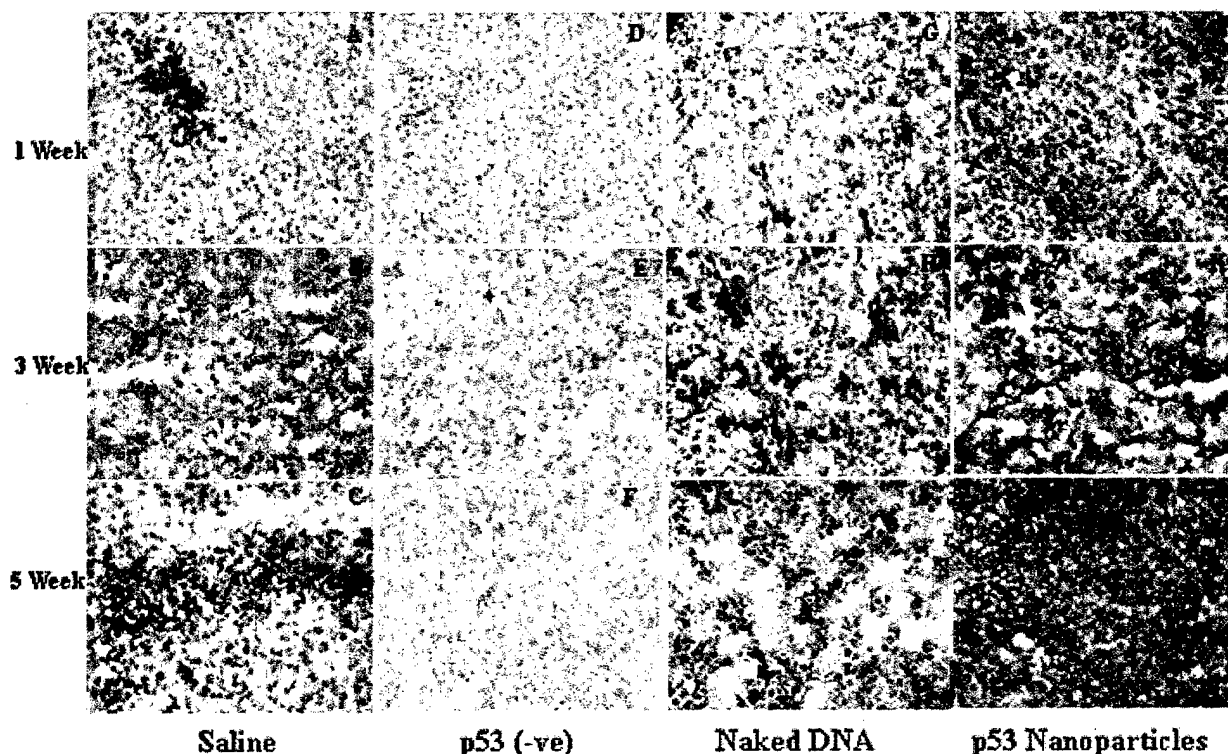

Figure 9. Immunohistochemistry of thrombospondin (TSP-1) in tumor tissue. A, D, G and J represent 1 week data for respective groups. B, E, H and K represent 3 week data for respective groups and C, F, I and L represent 5 week data for respective groups.

technique. Apoptosis was studied by DeadEnd™ TUNEL assay (Promega). Nanoparticle-mediated anti-tumor effect was found to be due to sustained induction of antiangiogenic protein thrombospondin I (TSP-1) expression (Fig 9) and higher induction of apoptosis (Fig 10). High expression of TSP-1 correlated with the significantly (p < 0.001) lower number of blood vessels (Fig 11, Table 1), thus that probably reduced the blood supply to the tumor tissue and inhibited the tumor growth.

Figure 10. Determination of apoptosis in tumor tissue. A, D, G and J represent 1 week data for respective groups. B, E, H and K represent 3 week data for respective groups and C, F, I and L represent 5 week data for respective groups. Arrows indicate apoptotic cells

Table 1: Effect of *wt*-p53-nanoparticles on blood vessel density in mice tumors

Time \ Treatment	1 Week	3 Week	5 Week
Saline	17.2 ± 4.9	25.1 ± 3.7	37.5 ± 6.8
p53 (-ve)-DNA-loaded Nanoparticles	22.1 ± 7.5	29.4 ± 6.8	47.2 ± 16.5
Wt-p53 Naked DNA	20.1 ± 3.5	21.1 ± 5.2	22.1 ± 6.1
Wt- p53-DNA-loaded Nanoparticles	11.4 ± 2.7*	6.0 ± 42**	5.0 ± 3.8#

N= 10, ANOVA single-factor analysis *p = 0.0001, **p < 0.00001, #p < 0.0001

References
1. Q. R. Chen, A. J. Mixson, *Front. Biosci.* **3**, D997-D1004 (Sep 15, 1998).
2. W. M. Gallagher, R. Brown, *Ann Oncol* **10**, 139-50 (Feb, 1999).
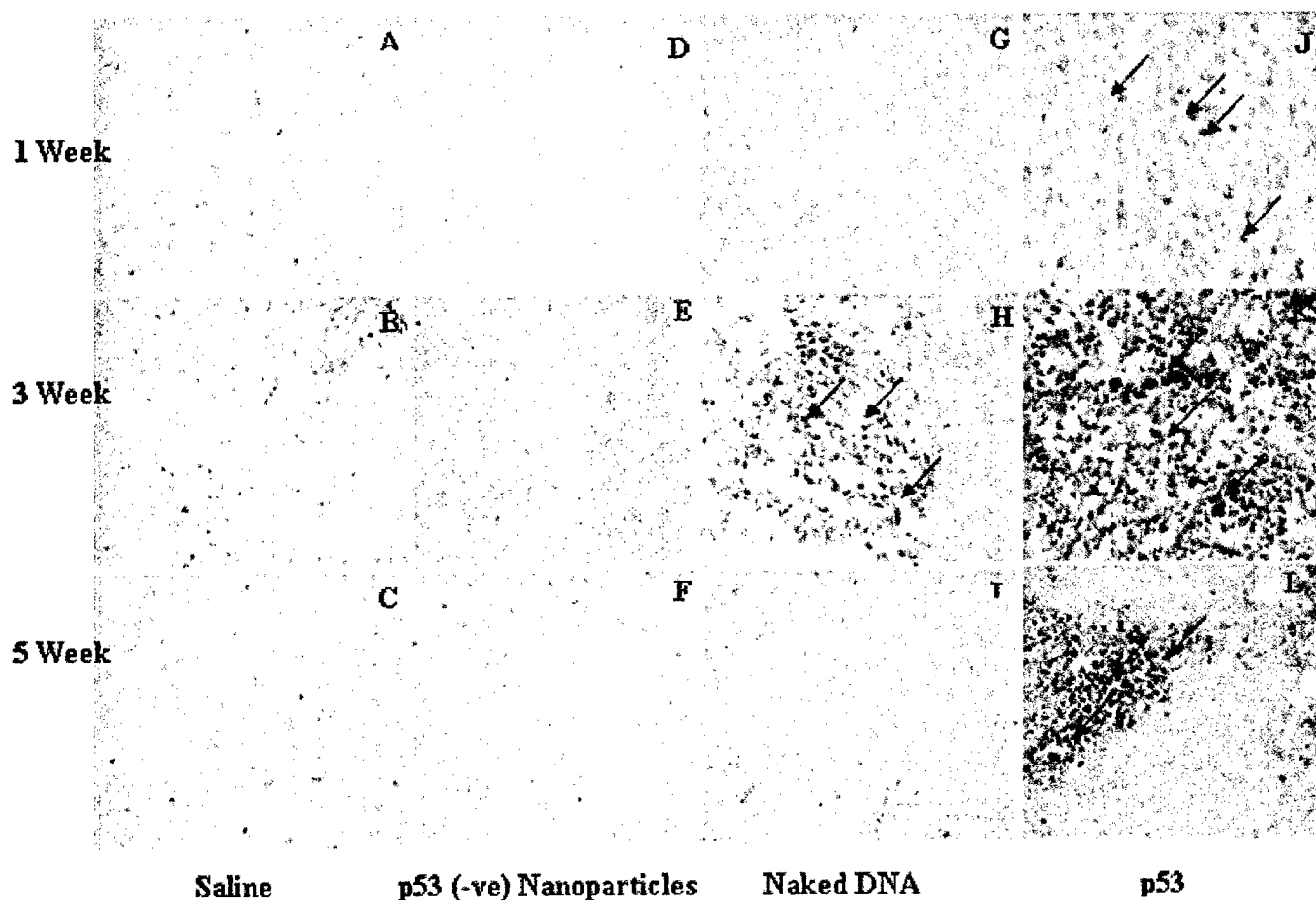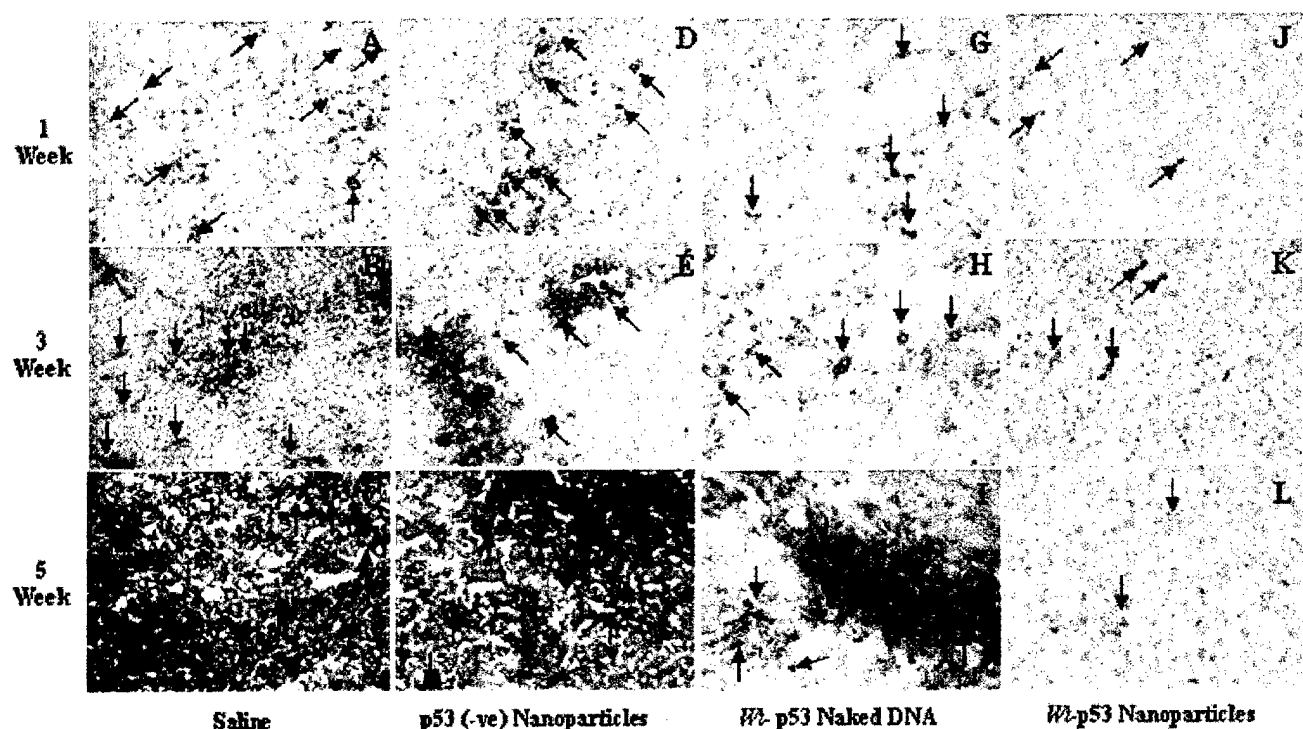
Figure 11. CD-31 staining to determine effect of various treatments on angiogenesis in tumor tissue. A, D, G and J represent 1 week data for respective groups. B, E, H and K represent 3 week data for respective groups and C, F, I and L represent 5 week data for respective groups. Arrows indicate the blood vessels

Key Research accomplishments during last year

1. p53-DNA-loaded nanoparticles were used to demonstrate sustained antiproliferative activity in human breast cancer cells. Also , the mechanism of sustained antiproliferative activity was studied by following the intracellular distribution of nanoparticles and DNA released from nanoparticles.
2. p53-DNA-loaded nanoparticles were investigated for sustained tumor inhibition in murine model of breast cancer and mechanism of nanoparticle-mediated anti-tumor effect was studied by immunohistochemistry and Real time PCR analysis of angiogenic proteins. Also, the effect of nanoparticles on apoptosis in tumor cells was investigated using TUNEL assay.

Reportable outcomes

1. **Received PhD in Pharmaceutical Sciences, 2004**
2. **Awards**
   * Norman and Bernice Harris award for excellence in cancer research (2002).
   * Widaman Fellowship Supplement (2002-2005).
   * "College of Pharmacy" Award for excellent Oral Presentation at Midwest Student Biomedical Research Forum, Omaha, NE (2003).
3. **Publications**
   * **Prabha, S.**, Zhou, W. Z., Panyam, J. and Labhasetwar, V. (2002) Particle size dependency of nanoparticle mediated gene transfection: Effect of particle size. Int J Pharm, 244 (1-2): 105-115.
   * Panyam, J., Zhou, W.Z., **Prabha, S.**, Sahoo, S. and Labhasetwar, V. (2002) Rapid endo-lysosomal escape of poly (D,L-lactide-co-glycolide) nanoparticles: implications for drug and gene delivery. FASEB J, 16(10): 1217-1226.
   * Sahoo, S. K., Panyam, J., **Prabha, S.** and Labhasetwar V. (2002) Residual polyvinyl alcohol associated with poly (DL-lactide-co-glycolide) nanoparticles affects their physical and cellular uptake properties. J Control Release, 82(10): 105-114.

9

* Panyam, J., Sahoo, S.K., **Prabha, S.** and Labhasetwar, V. (2003) Fluorescence and electron microscopy probes for poly(D,L-lactide-co-glycolide) nanoparticles. Int J Pharm, 262, 1-11.
* **Prabha, S.** and Labhasetwar, V. (2004) Critical determinants in nanoparticle-mediated gene expression. Pharm Res, 21 (2), 354-63.
* **Prabha, S.**, Ma, W., and Labhasetwar, V. (2004) Biodegradable Nanoparticles as Gene Expression Vector in Polymeric Gene Delivery: Principles and Applications edited by Mansoor Amiji, CRC Press. In Press.
* **Prabha, S.** and Labhasetwar, V. (2004) Nanoparticle-Mediated Wild Type-P53 Gene Delivery Results in Sustained Antiproliferative Activity in Breast Cancer Cells, Molecular Pharmaceutics In Press

3. **Presentations**
* Panyam, J., **Prabha, S.**, Sahoo S. K. and Labhasetwar, V. Evidence of Rapid Escape of Nanoparticles from Endosomes. Poster presentation at 5th International Symposium on Polymer Therapeutics: From Laboratory to Clinical Practice, Jan 2002, Cardiff, UK.
* Panyam, J., **Prabha, S.**, Sahoo, S. and Labhasetwar, V. Evidence of rapid escape of nanoparticles from endosomes. Poster presentation at 6th Annual Cardiovascular Research Symposium, University of Nebraska Medical Center, Feb 2002, Omaha, NE.
* Labhasetwar, V., Panyam, J., **Prabha, S.** and Sahoo, S.K.; Nanoparticles for Drug and Gene Delivery. Abstract # 196, Controlled Release 29th annual meeting proceedings; 2002, Seoul, South Korea.
* **Prabha, S.**, Panyam, J., and Labhasetwar, V. Fractionated DNA-Loaded Nanoparticles Show Different Levels of Gene Transfection In Vitro, oral presentation at 34th Annual Post-Graduate Scientific Research Meeting (PGSRM), June 2002, Omaha, NE.
* Panyam, J., **Prabha, S.**, Sahoo, S. K. and Labhasetwar, V. Selective Cationization of PLGA-Nanoparticles in Endo-Lysosomal Compartment Results in their Cytoplasmic Escape, oral presentation at 34th Annual Post-Graduate Scientific Research Meeting (PGSRM), June 2002, Omaha, NE.
* Sahoo S.K., Panyam, J., **Prabha, S.** and Labhasetwar, V., Residual Polyvinyl Alcohol Associated with Poly (DL-lactide-co-glycolide) Nanoparticles Affects their Physical Properties and Cellular Uptake, poster presentation at 34th Annual Post-Graduate Scientific Research Meeting (PGSRM), June 2002, Omaha, NE.
* **Prabha, S.** and Labhasetwar, V., Interfacial Properties influence Nanoparticle-Mediated Gene Expression, Oral Presentation at Midwest Student Biomedical Research Forum (MSBRF), Feb 2003, Omaha, NE.
* Panyam, J., **Prabha, S.**, Sahoo, S.K. and Labhasetwar, V. Selective cationization of PLGA nanoparticles in endo-lysosomal compartment results in their cytoplasmic escape. The 34th Annual Midwest Student Biomedical Research Forum, Feb 2003, Omaha, NE.
* **Prabha, S.** and Labhasetwar, V., Effect of residual polyvinyl alcohol on nanoparticle-mediated gene transfection, Poster presentation at The American Society of Gene Therapy (ASGT) 6th annual meeting, June 4-8, 2003, Washington, DC.
* **Prabha, S.** and Labhasetwar, V., Effect of polymer molecular weight and composition on nanoparticle-mediated gene transfection, Poster presentation at The American Society of Gene Therapy (ASGT) 6th annual meeting, June 4-8, 2003, Washington, DC.
* **Prabha, S.** and Labhasetwar, V., Effect of Polyvinyl Alcohol Concentration, Molecular Weight and Composition on Nanoparticle-mediated Gene Transfection, Podia presentation at 35th Annual Post-Graduate Scientific Research Meeting (PGSRM), June 2003, Chicago, IL.
* **Prabha, S.** and Labhasetwar, V., Effect of Polymer Molecular Weight and Composition on Nanoparticle-mediated Gene Transfection, Poster presentation at The 30th Annual Meeting and Exposition of Controlled Release Society, July 2003, Glasgow, Scotland, UK.

* **Prabha, S.** and Labhasetwar, V., Effect of Residual Polyvinyl Alcohol on Nanoparticle-mediated Gene Transfection in Breast Cancer Cells, Poster presentation at The 30th Annual Meeting and Exposition of Controlled Release Society, July 2003, Glasgow, Scotland, UK.
* **Prabha, S.** and Labhasetwar, V., Nanoparticle-Mediated Sustained Wild Type-P53 Gene Delivery Results In Greater Antiproliferative Activity In Breast Cancer Cells, Oral Presentation at Midwest Student Biomedical Research Forum (MSBRF), Feb 2004, Omaha, NE.

4. **Job:** "Formulation Scientist", Ferndale Labs, MI.

Conclusions

Nanoparticles demonstrated sustained gene expression, both *in vitro* and *in vivo*. Therapeutic efficacy of nanoparticles with tumor suppressor p53 gene in breast cancer mouse model was attributed to sustained gene expression in tumor tissue. In conclusion, the present study demonstrates the efficacy of biodegradable nanoparticles as a sustained gene expression system with potential applications in the therapy of breast cancer and other chronic disease conditions.

Critical Determinants in PLGA/PLA Nanoparticle-Mediated Gene Expression

Swayam Prabha[1] and Vinod Labhasetwar[1,2,3]

Purpose. The aim of the study was to determine the critical determinants in nanoparticle-mediated gene transfection. It was hypothesized that different formulation parameters could affect the nanoparticle characteristics and hence its gene transfection.

Methods. Nanoparticles encapsulating plasmid DNA encoding for firefly luciferase were formulated using polylactide (PLA) and poly (D,L-lactide-*co*-glycolide) (PLGA) polymers of different compositions and molecular weights. A multiple-emulsion solvent-evaporation method with polyvinyl alcohol (PVA) as an emulsifier was used to formulate DNA-loaded nanoparticles. Gene expression of nanoparticles was determined in breast cancer (MCF-7) and prostate cancer (PC-3) cell lines.

Results. Nanoparticles formulated using PLGA polymer demonstrated greater gene transfection than those formulated using PLA polymer, and this was attributed to the higher DNA release from PLGA nanoparticles. Higher-molecular-weight PLGA resulted in the formation of nanoparticles with higher DNA loading, which demonstrated higher gene expression than those formulated with lower-molecular-weight PLGA. In addition, the nanoparticles with lower amount of surface-associated PVA demonstrated higher gene transfection in both the cell lines. Higher gene transfection with these nanoparticles was attributed to their higher intracellular uptake and cytoplasmic levels. Further study demonstrated that the molecular weight and the degree of hydrolyzation of PVA used as an emulsifier also affect the gene expression of nanoparticles.

Conclusions. Results thus demonstrate that the DNA loading in nanoparticles and its release, and the surface-associated PVA influencing the intracellular uptake and endolysosomal escape of nanoparticles, are some of the critical determinants in nanoparticle-mediated gene transfection.

KEY WORDS: nonviral gene delivery; biodegradable and biocompatible polymers; sustained release; cancer therapy

INTRODUCTION

Toxicity and immunogenicity concerns associated with viral vectors have led to an active interest in nonviral vectors for gene delivery (1–3). Among the many nonviral systems currently being investigated, biodegradable polymeric nanoparticles with entrapped plasmid DNA have shown the potential for achieving sustained gene expression (4–6). Nanoparticles are colloidal particles in the nanometer size range and contain a plasmid DNA of interest entrapped in their polymer matrix (5). Although matrix-type nanoparticles have been formulated using different polymers (7), nanoparticles

[1] Department of Pharmaceutical Sciences, University of Nebraska Medical Center, Omaha, NE 68198.
[2] Department of Biochemistry, University of Nebraska Medical Center, Omaha, NE 68198.
[3] To whom correspondence should be addressed (email: vlabhase@unmc.edu).

formulated from poly(D,L-lactide-*co*-glycolide) (PLGA) and polylactide (PLA) are especially of interest for gene delivery because of their biocompatibility, biodegradability, and sustained-release characteristics.

We have previously studied the nanoparticle-mediated gene transfection both *in vitro* (6) and *in vivo* (8) and have also determined the influence of particle size of nanoparticles on gene transfection *in vitro* (5). Other groups have also investigated the transfection efficiency of gene-loaded PLGA nanoparticles in comparison to the naked DNA and liposomal formulations both *in vitro* and *in vivo* (4). However, the influence of various formulation parameters on gene transfection, which could be critical to enhancing the efficiency of nanoparticle-mediated gene transfection, has not been thoroughly examined before.

We have recently demonstrated that following their uptake into the cells through an energy-dependent endocytic process, PLGA-nanoparticles rapidly escape the endolysosomes into the cytoplasm (6). Nanoparticles are anionic at physiologic pH; however, in the acidic pH of endolysosomes, nanoparticles acquire a net positive charge. This cationization of nanoparticle surface selectively in the endolysosomal compartment is hypothesized to result in the localized destabilization of the endosomal membrane leading to escape of nanoparticles. In the transmission electron microscopy of the cell, nanoparticles were seen to interact with the endosomal vesicles only in the secondary endosomes, where pH is acidic (pH ~4), but not in the primary endosomes where the pH is 7.4. Furthermore, it was demonstrated that nanoparticles that do not show charge reversal with pH (e.g., polystyrene nanoparticles) were not seen to escape into the cytoplasmic compartment, thus substantiating our proposed hypothesis. The uptake of nanoparticles was inhibited in the presence of metabolic inhibitors (sodium azide and deoxyglucose), confirming the endocytic process of uptake of nanoparticles. The nanoparticle uptake was determined to be partly through fluid-phase pinocytosis and partly through clathrin-coated pits in vascular smooth muscle cells (6). Nanoparticles that escaped the endosomes into the cytoplasmic compartment are hypothesized to slowly release the entrapped DNA, resulting in sustained gene expression.

Recently, we have demonstrated that polyvinyl acetate (PVA), which is a commonly used emulsifier in the formulation of nanoparticles, remains associated with the nanoparticle surface. This occurs because the hydrophobic portion of PVA anchors into the nanoparticle matrix during their formulation, could not be washed away, and therefore forms the nanoparticle interface. Other investigators, with similar formulation of nanoparticles, have demonstrated the presence of PVA at the nanoparticle surface using x-ray photoelectron spectroscopy (9). PVA has been estimated to form multilayers around the nanoparticle surface (10). Our studies have demonstrated that the residual surface-associated PVA affects the physical properties of nanoparticles as well as their cellular uptake (11). Therefore, it was hypothesized that the surface-associated PVA and its concentration, type (degree of hydrolyzation), and molecular weight could influence the gene transfection of nanoparticles.

Thus, the factors influencing the intracellular uptake of nanoparticles and their distribution, and DNA loading in

nanoparticles and its release, could affect nanoparticle-mediated gene transfection. Therefore, the aim of the current study was to investigate the critical formulation determinants with an objective to enhancing nanoparticle-mediated gene transfection.

MATERIAL AND METHODS

Materials

Poly(D,L-lactide-co-glycolide) (PLGA) of different molecular weights (50:50 lactide/glycolide, Mw 12 kDa, 53 kDa, and 143 kDa), and composition (PLGA 75:25, PLGA 50:50, Mw 53 kDa) and Poly(D,L-lactide) (PLA, Mw 53 kDa) were purchased from Birmingham Polymers, Inc. (Birmingham, AL). Acetylated bovine serum albumin (Ac-BSA) and polyvinyl alcohol (PVA, average Mw 30–70 kDa) were purchased from Sigma Chemical Co. (St. Louis, MO). PVA with different molecular weights (87–89% hydrolyzed, average Mw 13–23 kDa, 31–50 kDa, and 85–146 kDa) and degree of hydrolyzation (average Mw 9–10 kDa, 80% and 87–89% hydrolyzed) were purchased from Aldrich Chemical Co. (Milwaukee, WI). 6-Coumarin was purchased from Polyscience Inc. (Warrington, PA). Fetal bovine serum (FBS, heat inactivated), 1× trypsin-EDTA, Rosewell Park Memorial Institute 1640 (RPMI 1640) medium, and penicillin-streptomycin were obtained from Gibco-BRL (Grand Island, NY). Human breast carcinoma (MCF-7) and human prostate cancer (PC-3) cells were purchased from American Type Culture Collection (ATCC) (Manassas, VA). Luciferase plasmid with simian virus 40 (SV40) promoter and cytomegalovirus (CMV) enhancer (pGL3), cell culture lysis reagent (CCLR, 5×), luciferase assay kit, and the recombinant luciferase protein were purchased from Promega (Madison, WI). Fu-GENE™ 6 was purchased from Roche Diagnostics, Indianapolis, IN. Mitochondria/cytosol fractionation kit was purchased from BioVision Inc. (Mountain view, CA). All other chemicals and reagents were purchased from Fisher Scientific (Pittsburgh, PA).

Methods

Plasmid Preparation and Formulation of Nanoparticles Containing Plasmid DNA

Plasmid DNA encoding for luciferase gene (pGL3, with SV40 promoter and enhancer) was prepared using Qiagen® mega/giga column (Qiagen, CA). In brief, plasmid DNA was propagated in *E. coli* strain DH5α under defined growth conditions. The bacterial colonies containing plasmid DNA were selected, and DNA was extracted and purified using an ion-exchange resin column.

DNA-loaded nanoparticles were formulated using a double-emulsion solvent-evaporation technique as described by Prabha *et al.* (5). In brief, in a typical procedure, DNA solution (1 mg of DNA + 2 mg of nuclease-free acetylated BSA dissolved in 200 μl of TE buffer) was emulsified into a polymer solution (30 mg/ml) by sonication for 2 min using a probe sonicator at 55 W energy output (Sonicator® XL, Misonix, NY) to form a water-in-oil emulsion. Acetylated BSA was incorporated in the formulation because it is nuclease-free and hence is not expected to degrade DNA. BSA was

used in the formulation to facilitate the release of DNA. The above emulsion was further emulsified into 6 ml of aqueous solution of PVA (concentration of PVA depends on the protocol) using the sonicator as above for 5 min to form a water-in-oil-in-water emulsion. The emulsion was stirred overnight to evaporate chloroform, and the nanoparticles thus formed were recovered by ultracentrifugation (35,000 rpm for 20 min at 4°C, Optima™ LE-80K, Beckman, Palo Alto, CA), washed twice to remove PVA and unentrapped DNA, resuspended in sterile water, and lyophilized for about 48 h.

For the cellular uptake studies, nanoparticles containing fluorescent marker in addition to DNA were prepared by dissolving 6-coumarin, a fluorescent dye (50 μg), in the polymer solution before emulsification. As reported in our previous studies, the incorporated dye acts a probe for nanoparticles without changing their physical properties (5).

Physical Characterization of Nanoparticles

Particle size and polydispersity of nanoparticles (0.5 mg/ml nanoparticles in distilled water) was determined using a Zeta Plus™ particle size analyzer (Brookhaven Instruments Corp., Holtsville, NY). The ζ potential (surface charge) of nanoparticles (0.5 mg/ml nanoparticles in distilled water) was determined using a Zeta Plus™ ζ potential analyzer. DNA loading in nanoparticles was determined from the total amount of DNA added in the formulation and the DNA amount that was not encapsulated. For this, the concentration of DNA in the washings was determined by measuring the UV absorbance at 260 nm with the washings from the control nanoparticles formulated without DNA as a blank. The amount of DNA loaded in the nanoparticles was calculated from the standard curve of DNA prepared in washing solution obtained from control nanoparticles. The standard curve was prepared in the washing from the control nanoparticles so that BSA that is not encapsulated and is present in the washing does not interfere in the calculation of DNA concentration. The amount of PVA associated with nanoparticles was determined using a colorimetric method as described in our previous publication (11).

DNA release from nanoparticles under *in vitro* conditions was studied by incubating 0.15 mg of the respective formulation of nanoparticles with 0.5 ml of TE buffer in Eppendorf® tubes at 37°C in an Environ Orbital Shaker (Lab Line, Melrose Park, IL) set at 100 rpm. Separate tubes were used for each data point. At predetermined time intervals, the nanoparticle suspension was centrifuged, and the amount of DNA released in the supernatant was analyzed by Pico-Green® assay (Promega). Previous studies have demonstrated that the DNA encapsulated and that released from nanoparticles maintained their conformation, suggesting that the homogenization conditions used in our studies do not cause fragmentation of DNA (5).

Transfection Studies and Determination of Luciferase Protein Levels

MCF-7 and PC-3 cells were grown in RPMI medium supplemented with 10% FBS, 100 μg/ml penicillin G, and 100 μg/ml streptomycin. For transfection studies, cells were cultured at the seeding density of 35,000 cells/ml/well in 24-well plate 1 day before transfection. A nanoparticle suspension

was prepared in the serum-free medium (4 mg in 500 μl) using a water bath sonicator for 10 min (FS140, Fisher Scientific, Pittsburgh, PA). The nanoparticle suspension was then diluted to 9 ml with complete RPMI 1640 medium. The medium in the wells was replaced with 1 ml of nanoparticle suspension. Thus, the dose of nanoparticles per well was 444 μg/ml. The dose of nanoparticles used for the transfection was based on the preliminary dose–response study. Because the dose of nanoparticles was kept constant, the DNA dose per well varied and depended on the DNA loading in the respective formulation (Tables I and II). Medium was changed 1 day after the transfection with no further addition of nanoparticle dose. Medium was replaced on every alternate day thereafter. Cells were lysed at 1, 3, 5, and 7 days in the case of MCF-7 cells and at 3 days in the case of PC-3 cells. To measure luciferase protein levels, cells were washed twice using 1× phosphate-buffered saline (PBS) and lysed using 1× CCLR (Promega). To each 20 μl of the cell lysate sample, 100 μl of the reconstituted luciferase assay substrate (Promega) was added, and the chemiluminiscence intensity was measured immediately using a luminometer (TD 20/20, Promega). The amount of luciferase protein was determined from the standard plot prepared using a recombinant luciferase protein. The total cell protein was determined using a BioRad® protein assay kit (BioRad, Hercules, CA), and the data were represented as luciferase protein levels (pg/mg cell protein). Transfection studies with naked DNA (11.8 μg/ml/well) and naked DNA + PVA (PVA amount 16.7 μg/ml/well) were carried out as controls. The dose of PVA used for the above transfection study was calculated from the amount of PVA associated with the dose of nanoparticles used for transfection for the formulation prepared using 143-kDa polymer and 2% PVA solution as an emulsifier. Transfection with plasmid DNA (11.8 μg DNA/well/ml) using FuGENE™ 6 was carried out similar to that used for nanoparticles except that the transfection was carried out in the absence of serum as per the manufacturer's instructions. A 1:3 complex of plasmid DNA: FuGENE™ 6 was prepared in a serum-free medium, and the complex was then added to the cells. The medium was changed 1 day following the addition of the complex and on every alternate day thereafter.

Cellular Nanoparticle Uptake

For the cellular uptake study, a formulation of DNA-loaded nanoparticles containing 6-coumarin as a fluorescent marker was used. MCF-7 cells were incubated with a suspension of nanoparticles at the same dose used for the transfection study for 1 h, washed twice with 1× PBS, and then lysed using 100 μl/well of 1× CCLR. A 5-μl aliquot of each sample was used to determine the total cell protein using BioRad® assay, and the remaining portion was lyophilized for 24 h. The dye (6-coumarin) from the nanoparticles in the cell lysate was extracted by incubating each cell lysate sample with 1 ml of methanol at 37°C for 24 h at 100 rpm in an Environ® lab shaker (Labline, Melrose Park, IL). The samples were centrifuged (14,000 rpm for 10 min at 4°C in an Eppendorf® microcentrifuge) to remove the cell debris, and the supernatant from each sample was analyzed for the 6-coumarin levels using a high-performance liquid chromatography (HPLC) as described in our previous studies (12). A standard plot using different amounts of nanoparticles dispersed in 1× CCLR and

treated similarly to cell lysate was used to quantify the nanoparticle levels. The uptake was represented as nanoparticle amount (μg/mg total cell protein).

Cell Fractionation

About 3×10^5 MCF-7 cells/well were seeded in six-well plates and incubated at 37°C, 5% CO_2 for 1 day. A suspension of nanoparticles containing fluorescent dye (888 μg/2 ml/well) was added to the cells and incubated at 37°C and 5% CO_2. The concentration of nanoparticle used in this study was the same as that used for the transfection studies. The medium was changed 1 day after incubation of cells with nanoparticles, and no further dose of nanoparticle was added. Medium was changed on every alternate day thereafter. At different time intervals (1 h, 8 h, 1 day, 3 days, 5 days, and 7 days), cells were trypsinized and harvested by spinning at 1000 rpm for 10 min, washed twice with 1× phosphate-buffered saline (PBS), and suspended in 1× cytosol extraction buffer containing dithiothreitol (DTT) and protease inhibitor cocktail (BioVision, Mountain View, CA). The cells were then homogenized using a pellet pestle® motor (Fisher) and centrifuged at $700 \times g$ to collect the supernatant that contained the cytosol fraction. The supernatant was then lyophilized, and the dye from the nanoparticles was extracted using methanol as above. The samples were then analyzed for the nanoparticle levels using HPLC as described above. A standard curve was constructed using different concentrations of nanoparticles under identical conditions that were used for analysis of nanoparticle levels in cell lysate to quantify the amount of nanoparticles present in the cell fraction.

Statistical Methods

Student *t*-test was used to test the significance of difference in the transfection efficiency and uptake of the smaller and the larger-sized particles. A p value less than 0.05 was accepted as statistically significant. All data analyses were done using Minitab® statistical software (Minitab Inc., State College, PA).

RESULTS

Effect of Polymer Molecular Weight and Composition on Physical Properties and Gene Transfection of Nanoparticles

In general, DNA loading, intracellular uptake of vector, and DNA release from the vector are some of the factors that govern gene transfection mediated by polymeric nonviral gene delivery systems. Therefore, the DNA-loaded nanoparticles using polymers of different compositions and molecular weights were formulated and characterized for physical properties and gene transfection *in vitro*. Molecular weight of PLGA was found to affect the DNA entrapment in nanoparticles, with greater efficiency of DNA encapsulation observed in the nanoparticles formulated using higher-molecular-weight PLGA (143 kDa) (Table I). Particle size of the nanoparticles formulated using higher-molecular-weight polymer was smaller; the particles formed were more uniform in size as indicated by lower polydispersity index, and these particles had relatively lower negative ζ potentials as compared to those formulated using lower-molecular-weight polymers (Table I). The residual PVA associated with the nanoparticle

Table I. Physical Characterization of the Nanoparticles Formulated Using PLGA/PLA of Different Molecular Weights and Compositions

Formulation parameter	Polymer molecular weight (kDa)	Polymer composition (lactide: glycolide ratio)	PVA bound to nanoparticles (%w/w)*	Mean particle size (nm)*	Polydispersity index*	ζ potential (mV)**	DNA loading (mg/100 mg nanoparticles)	DNA dose (μ/ml/well) used for transfection
Effect of molecular weight of PLGA	12	50:50	2.3 ± 0.9	563 ± 6	0.25 ± 0.02	−17.8 ± 1.0	1.8	8.0
	53	50:50	2.2 ± 0.3	685 ± 40	0.32 ± 0.02	−16.6 ± 1.4	1.7	7.5
	143	50:50	3.8 ± 0.4	375 ± 22	0.19 ± 0.01	−11.5 ± 3.4	2.9	12.9
Effect of polymer composition	53	100:0	2.4 ± 0.3	571 ± 9	0.21 ± 0.02	−14.3 ± 1.7	1.8	8.0
	53	75:25	2.2 ± 0.2	485 ± 11	0.23 ± 0.01	−16.6 ± 1.4	1.9	8.4
	53	50:50	2.2 ± 0.3	685 ± 40	0.32 ± 0.03	−18.2 ± 3.8	1.7	7.5

* Data represented as mean ± SEM, *n = 3, **n = 5.

Table II. Physical Characterization of the Nanoparticles Formulated Using Different PVA

Formulation parameter	PVA concentration (%)	PVA average molecular weight (kDa)	PVA degree of hydrolyzation (%)	PVA bound to nanoparticles (%w/w)*	Mean particle size (nm)*	Polydispersity index*	ζ potential (mV)**	DNA loading (mg/100 mg nanoparticles)	DNA dose (μ/ml/well) used for transfection
Effect of PVA concentration	0.5	31–50	88	2.2 ± 0.2	693 ± 2	0.3 ± 0.04	−31.3 ± 1.6	1.1	4.8
	2.0	31–50	88	3.8 ± 0.4	347 ± 3	0.2 ± 0.02	−11.5 ± 3.4	2.9	12.9
	5.0	31–50	88	5.2 ± 0.7	270 ± 1	0.2 ± 0.01	−6.5 ± 1.7	2.9	12.9
Effect of PVA molecular weight	2.0	13–23	88	5.7 ± 0.2	561 ± 22	0.17 ± 0.02	−15.6 ± 5.8	2.4	10.7
	2.0	31–50	88	4.1 ± 0.3	560 ± 3	0.21 ± 0.04	−17.3 ± 5.3	1.8	8.0
	2.0	83–146	88	3.7 ± 0.6	1207 ± 30	0.26 ± 0.04	−14.9 ± 4.7	1.9	8.4
Effect of PVA degree of hydrolyzation	2.0	13–23	80	9.1 ± 0.9	344 ± 30	0.21 ± 0.01	−22.2 ± 1.8	1.3	5.8
	2.0	13–23	89	5.7 ± 0.2	561 ± 22	0.17 ± 0.02	−15.6 ± 5.8	2.4	10.7

* Data represented as mean ± SEM, *n = 3, **n = 5.

surface was higher for the nanoparticles formulated using higher-molecular-weight PLGA (Table I). Furthermore, the DNA release from the nanoparticles formulated using higher-molecular-weight polymer was relatively higher than that from the nanoparticles formulated using lower-molecular-weight polymers (Fig. 1a). Transfection studies demonstrated that gene expression of nanoparticles increased with an increase in molecular weight of polymer used in their formulation. Nanoparticles formulated using PLGA of molecular weight 143 kDa demonstrated 50- to 100-fold, and the nanoparticles formulated using 53-kDa polymer demonstrated approximately 6- to 15-fold greater gene transfection, in comparison to the nanoparticles formulated using 12-kDa molecular weight polymer in MCF-7. In addition to the particle size, molecular weight of the polymer seems to play a role because the nanoparticles formulated with 53-kDa and 12-kDa polymers have similar particle size, DNA loading, and ζ potential, but the transfection with nanoparticles formulated with higher-molecular-weight polymer was higher than that of nanoparticles formulated with lower-molecular-weight polymer. Similar relatively higher gene transfection was observed in PC-3 cells for the nanoparticles formulated using higher-molecular-weight polymer than the gene transfection with the nanoparticles formulated using lower-molecular-weight polymers (Fig. 1c).

Gene transfection with an equivalent dose of naked DNA was about 50-fold lower than the gene transfection with the nanoparticles formulated using 143-kDa molecular weight PLGA in MCF-7 cells (Fig. 1b). Gene transfection with Fu-GENE™ 6, a commercially available transfection agent, was relatively higher than the gene transfection with nanoparticles in MCF-7 cells; however, the transfection level declined almost exponentially with time in case of the transfection agent (Fig. 2), whereas the level remained sustained with nanoparticles (Fig. 1b).

In further studies, the effect of polymer composition (lactide to glycolide ratio) on nanoparticle characteristics and gene transfection was studied. Nanoparticles were formulated using PLA (100% lactide) and PLGA of different compositions (lactide to glycolide ratio 75/25, 50/50) having an average molecular weight of about 53 kDa. Although the polymer composition did not show significant differences in the physical characteristics of nanoparticles (Table I), the cumulative DNA release from the nanoparticles formulated using PLA was relatively lower than that from the other two formulations of nanoparticles (Fig. 3a). Nanoparticles formulated using PLA demonstrated significantly lower gene transfection as compared to gene transfection with the nanoparticles formulated using polymers containing glycolide in part (PLGA) in both MCF-7 (Fig. 3b) and PC-3 (Fig. 3c) cells.

Effect of Emulsifier (PVA) Concentration on Physical Properties, Transfection, Cellular Uptake, and Intracellular Distribution of Nanoparticles

Nanoparticle surface characteristic is a critical determinant because it determines the interaction of nanoparticles with the cell surface. It has been known that a fraction of PVA remains associated with PLGA and PLA nanoparticles and forms an interface (11,13). In order to study the effect of surface-associated PVA on gene transfection, nanoparticles (PLGA 50/50, molecular weight 143 kDa) were formulated
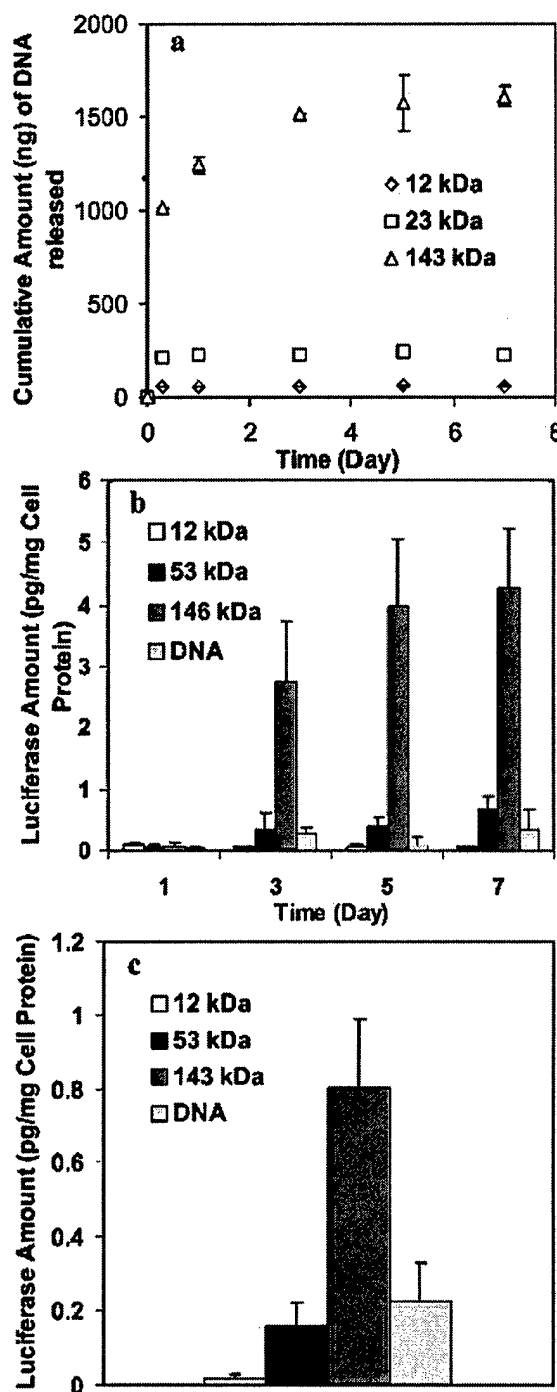

Fig. 1. Effect of molecular weight of PLGA on (a) *in vitro* release of DNA from nanoparticles and transfection of nanoparticles in (b) MCF-7 and (c) PC-3 cells. Cells (35,000 per well in 24-well plate) were incubated with nanoparticles (444 μg/ml/well, see Table I for dose of DNA) for 1 day after which the medium in the wells was replaced with fresh medium (without nanoparticles). Medium was changed on alternate days thereafter. Nanoparticles showed sustained gene transfection in MCF-7 cell line. In PC-3 cells, transfection was determined at the end of 3 days postincubation with nanoparticles. Studies in PC-3 could not be continued beyond 3 days because the cells reached confluency. Figure legend represents molecular weight of PLGA. Data as mean ± SEM, n = 6.
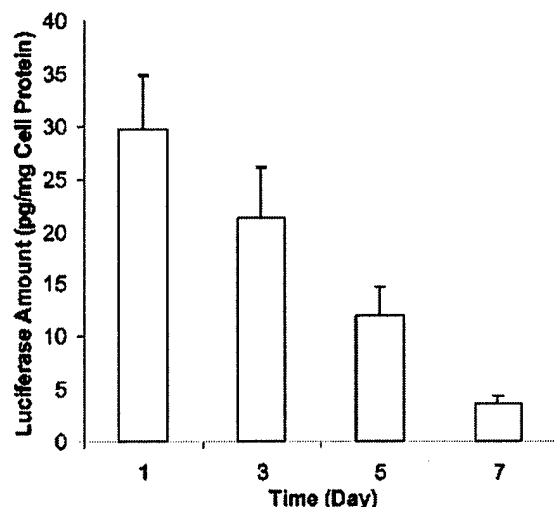
Fig. 2. Transfection with FuGENE™ 6. Plasmid DNA: FuGENE™ 6 (1:3) complex (DNA dose ~11.8 μg/ml/well) was prepared in serum-free medium, and the complex was added onto the cells (35,000 cells/well in 24-well plate). The medium in the wells was changed to the regular serum-containing medium at 24 h, and the luciferase protein levels were analyzed at the end of 1, 3, 5, and 7 days posttransfection. Data represented as mean ± SEM, n = 6.

using PVA (average molecular weight 31–50 kDa and 89% degree of hydrolyzation) at different concentrations. Although the particle size was reduced with the increase in PVA concentration, the nanoparticle-surface-associated PVA increased (Table II). PVA bound to the nanoparticle surface was found to affect the interfacial properties of nanoparticles, especially the surface charge, since the nanoparticles with higher amount of surface associated PVA had reduced anionic charge (Table II). DNA loading in the nanoparticles formulated with lower concentration of PVA (0.5% w/v) was lower than that in the nanoparticles formulated using 2% and 5% w/v PVA (Table II).

To study the effect of surface-associated PVA on gene expression, nanoparticles formulated using 2% w/v and 5% w/v PVA concentration were used for comparison as these formulations had almost similar DNA loading and particle size. Nanoparticles with lower amounts of surface-associated PVA demonstrated 12- to 20-fold higher gene transfection in MCF-7 cells than those with higher amount of surface-associated PVA (Fig. 4b). Similar higher transfection was observed in PC-3 cell line for the nanoparticles formulated using 2% w/v PVA; however, the difference in the transfection was only twofold in this cell line (Fig. 4c).

Despite relatively lower DNA loading in the nanoparticles formulated with 0.5% w/v PVA than that in the nanoparticles formulated with 5% w/v PVA, gene transfection of the nanoparticles formulated with 0.5% w/v PVA was 1.5- to 3-fold higher as compared to the gene transfection of the nanoparticles formulated with 5% PVA in MCF-7 cells. However, the gene transfection of the nanoparticles formulated with 2% w/v PVA was 10- to 20-fold greater than the gene transfection of the nanoparticles formulated with 5% PVA despite similar DNA loading. To demonstrate that the difference in the gene expression observed with different formulations of nanoparticles was caused by the effect of surface-
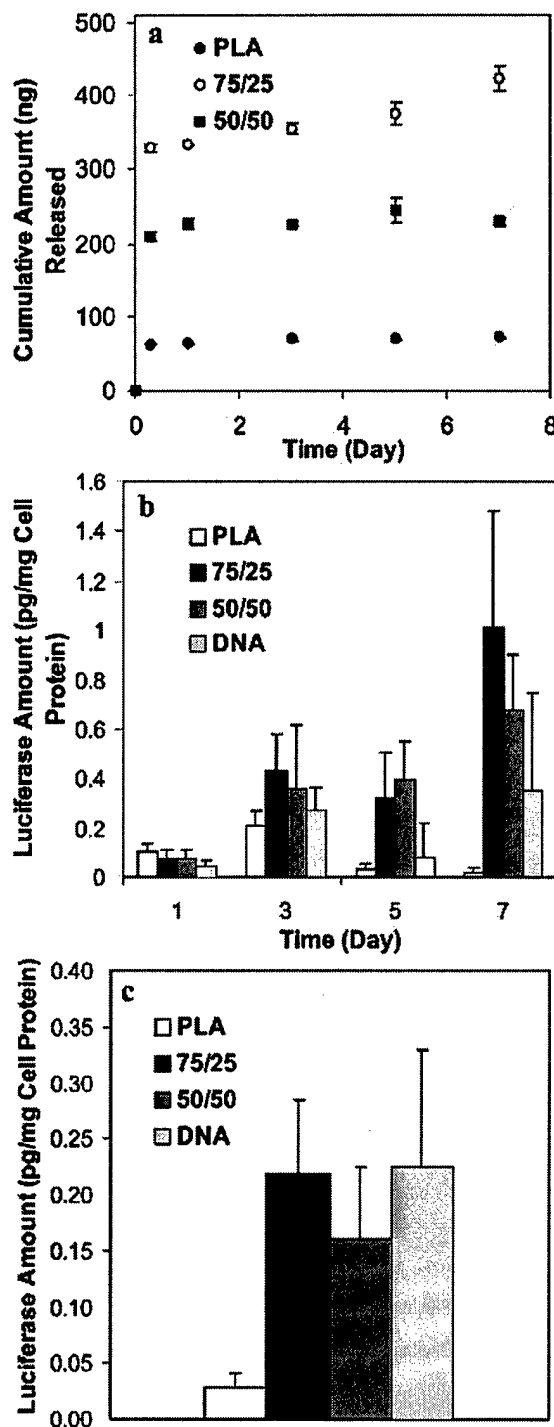

Fig. 3. Effect of polymer composition on (a) *in vitro* DNA release from nanoparticles and transfection of nanoparticles in (b) MCF-7 and (c) PC-3 cells. Cells (35,000/well in 24-well plate) were incubated with nanoparticles (444 μg/ml/well) for 1 day, and then the medium was replaced with fresh medium (without nanoparticles). Medium was changed on every alternate day thereafter, and transfection levels were determined at 1, 3, 5, and 7 days posttransfection in MCF-7 cell line and at 3 days posttransfection in PC-3 cell line. Figure legend represents lactide:glycolide ratio. Data shown as mean ± SEM, n = 6.
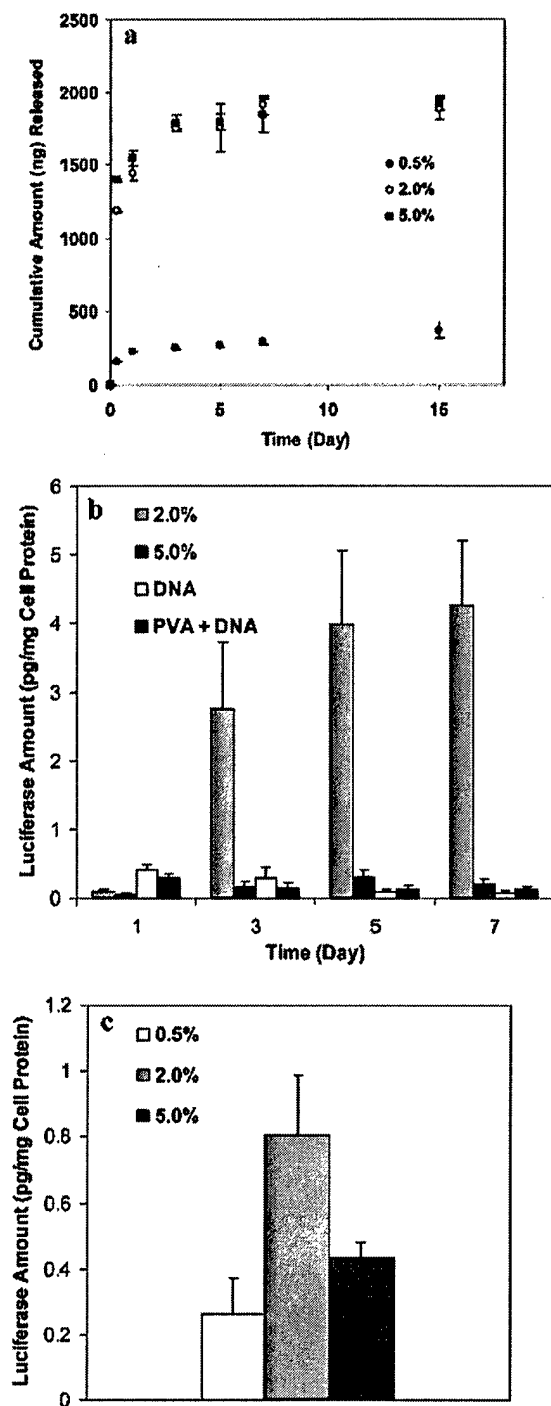
Fig. 4. Effect of PVA concentration on (a) *in vitro* release of DNA from nanoparticles and transfection of nanoparticles in (b) MCF-7 and (c) PC-3 cells. Cells (35,000 per well in 24-well plate) were incubated with nanoparticles (444 μg/ml/well, see Table II for dose of DNA) for 1 day, and then the medium in wells was replaced with fresh medium (without nanoparticles). Medium was changed on every alternate day thereafter, and luciferase protein levels were determined at 1, 3, 5, and 7 days posttransfection in MCF-7 cell line and at 3 days posttransfection in PC-3 cell line. Figure legend represents lactide:glycolide ratio. Identical protocol was used to determine transfection of plasmid DNA or plasmid DNA + PVA. Data shown as mean ± SEM, n = 6. Figure legend represents concentration of PVA used as an emulsifier. Data shown as mean ± SEM, n = 6.

associated PVA, a control experiment with plasmid DNA and plasmid DNA mixed with PVA was carried out. There was no significant difference in the transfection levels of DNA and DNA + PVA ($p > 0.05$) (Fig. 4b).

In order to account for the difference in the transfection of the two formulations of nanoparticles (prepared using 2% and 5% w/v PVA) despite similar DNA loading and release (Fig. 4a), the cellular uptake of the above two formulations of nanoparticles was determined. The results demonstrated a 1.5-fold higher uptake for the nanoparticles prepared using 2% w/v PVA as compared to that for the nanoparticles formulated using 5% w/v PVA (26 ± 1.4 μg nanoparticles/mg cell protein for 2% w/v PVA vs. 17.5 ± 1 μg nanoparticles/mg cell protein for 5% w/v PVA). Further analysis of the intracellular distribution of nanoparticles demonstrated that the nanoparticles formulated with 2% w/v PVA had over two-fold higher cytoplasmic levels than the nanoparticle levels for those formulated with 5% w/v PVA (Fig. 5). The cytoplasmic nanoparticle levels increased with incubation time, but these levels dropped gradually once the medium was changed after 1 day.

Effect of PVA Molecular Weight and Degree of Hydrolyzation on Physical Properties and Transfection of Nanoparticles

Because the surface-associated PVA was found to have a significant effect on the transfection of nanoparticles, further studies were carried out with the nanoparticles formulated using PVA of different molecular weights and degrees of hydrolyzation. In initial studies, nanoparticles were formulated (PLGA 50/50, molecular weight 143 kDa) using PVA of molecular weight 13–23 kDa but differing in the degree of hydrolyzation (80% and 89%). With the increase in degree of hydrolyzation of PVA, the DNA loading in nanoparticles increased (Table II), the surface-associated PVA was reduced, and gene transfection of nanoparticles was enhanced (Fig. 6a). Furthermore, the amount of DNA released from the nanoparticles formulated using PVA with higher (89%) degree of hydrolyzation was relatively greater than that from the nanoparticles formulated using PVA with lower (80%) degree of hydrolyzation (640 ± 40 ng vs. 360 ± 40 ng cumulative DNA release at the end of 7 days).

In a second set of experiments, nanoparticles were formulated (PLGA 50/50 of molecular weight 143 kDa) using PVA with the same degree of hydrolyzation (89%) but differing in molecular weight. Nanoparticle size was greater for the formulation prepared with high-molecular-weight PVA as compared to that prepared using lower-molecular-weight PVA (Table II). Also, the nanoparticles formulated with lower-molecular-weight PVA had relatively higher DNA loading. Despite relatively higher DNA loading and similar DNA release (643 ± 78 ng cumulative DNA release at the end of 7 days for 13- to 23-kDa PVA vs. 689 ± 27 ng for 31- to 50-kDa PVA vs. 636 ± 30 ng for 85- to 146-kDa PVA), the nanoparticles formulated using PVA of lower molecular weight (13–23 kDa) showed lower transfection levels than those formulated using PVA of molecular weight 31–50 kDa and 85–146 kDa (Fig. 6b).

DISCUSSION

Gene expression using nonviral vectors depends on several factors including efficient intracellular uptake of the ex-
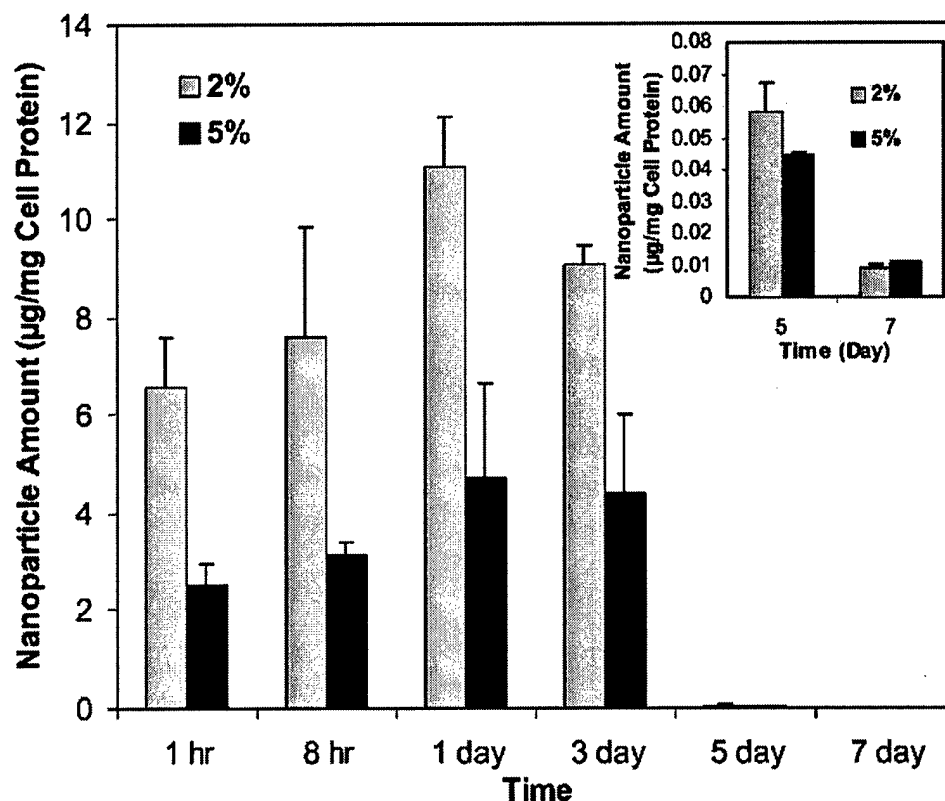
Fig. 5. Cytoplasmic levels of nanoparticles formulated using different concentrations of PVA in MCF-7 cells. Cells (3 × 10⁵ in 6-well plates) and the nanoparticle levels in the cytoplasm were determined at 1 h, 8 h, and 1 day postincubation. Medium was changed at 1 day with no further addition of nanoparticles and on every alternate day thereafter. Cytoplasmic nanoparticle levels were then determined at 3, 5, and 7 days postnanoparticle incubation. Inset shows the cytoplasmic levels of nanoparticles at 5 and 7 days of post-nanoparticle incubation. Data shown as mean ± SEM, n = 6.

pression vector, their escape from the degradative environment inside the endolysosomal compartment, dissociation of DNA from the vector, and the effective localization of DNA into the nucleus (3). Although different strategies are being investigated to overcome the barriers associated with gene delivery, the efficiency of gene expression with nonviral vectors remains relatively lower (14). Among several nonviral vectors, cationic polymers and lipid–DNA complexes are relatively more efficient; however, toxicity concerns and instability of these systems in the presence of serum limit their effective use for *in vivo* applications (14,15). Different approaches are being investigated to overcome the problems associated with the above systems (16,17).

Nanoparticles and microparticles formulated using PLGA and PLA polymers are recently being investigated as a nonviral gene delivery system because of their sustained release characteristics, biocompatibility, and biodegradability, and their ability to protect DNA from degradation in endolysosomes (4–6,18). Although PLGA/PLA nanoparticles are extensively investigated for drug and protein delivery (19), their application as a gene expression vector is recent. Our recent studies demonstrated that nanoparticles are internalized efficiently into cells, following which a fraction of them rapidly escapes the endolysosomes into the cytoplasm compartment (6). Escape of the expression vector from the endolysosomal compartment is an important characteristic

because most of the DNA degrades rapidly in this compartment (20).

In our studies, nanoparticle-mediated gene transfection increased with the increase in molecular weight of polymer, which could be explained based on relatively higher DNA loading and its release from the nanoparticles formulated with higher-molecular-weight polymer. Higher DNA loading in these nanoparticles could be related to the higher viscosity and better emulsifying properties of the polymer solution. This could have resulted in the formation of a more stable emulsion and, therefore, lower diffusion of DNA from the particles during the formulation step (21). It has been shown previously that the increase in the viscosity of the oil phase in the multiple emulsion leads to restricted movement of the water droplets inhibiting droplet coalescence and DNA loss that occur during the formation of secondary emulsion (21–23). The better emulsifying properties of higher-molecular-weight polymer are also evident from the lower particle size and more uniform particle size distribution data (Table I). Higher DNA release from the nanoparticles formulated using higher-molecular-weight PLGA could be explained based on the higher DNA loading in these nanoparticles (24). Higher DNA loading in nanoparticles probably leads to the formation of pores and channels as DNA is released initially, leading to further release of DNA through the channels formed. Thus, the relatively higher gene transfection observed with
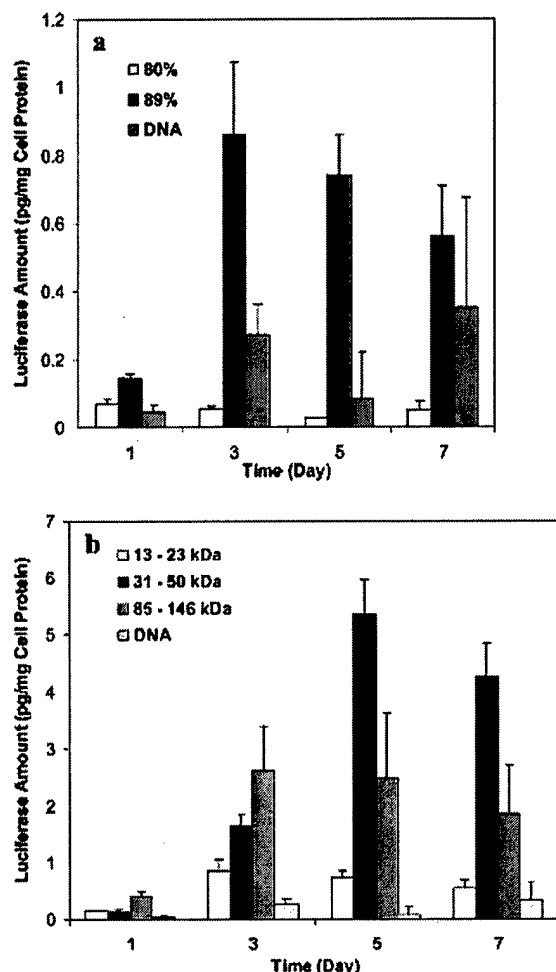
Fig. 6. Effect of (a) degree of hydrolyzation and (b) molecular weight of PVA used in the formulation of nanoparticles on transfection in MCF-7 cell line. Cells (35,000 per well in 24-well plate) were incubated with nanoparticles (444 μg/ml/well, see Table II for dose of DNA) for 1 day, and then medium was replaced with fresh medium (without nanoparticles). Medium was changed on every alternate day thereafter, and luciferase protein levels were determined at 1, 3, 5, and 7 days posttransfection in MCF-7 cell line. Data shown as mean ± SEM, n = 6.

the nanoparticles formulated with higher-molecular-weight polymer is related to the greater amount of DNA available to the cells for transfection.

Higher gene expression observed with 143-kDa PLGA nanoparticles as compared to plasmid DNA suggests that nanoparticles probably facilitate the internalization of DNA as well as protect it from degradation during their passage through the endolysosomal compartment into the cytoplasm. Sustained gene expression observed with nanoparticles suggests that the DNA is released slowly from the nanoparticles localized in the cytoplasmic compartment, which is then localized into the nucleus. In contrast, the gene expression with FuGENE™ 6, a commercially available transfection reagent (for *in vitro* transfection only), rapidly declines with time (Fig. 2), thus confirming the ability of nanoparticles to sustain gene expression. Sustained gene transfection achieved with nanoparticles could be beneficial in chronic disease conditions that

require low levels of protein expression for longer intervals of time (25).

Polymer composition was also found to affect the transfection properties of nanoparticles. In general, polymers with a higher proportion of lactic acid are more hydrophobic than those with a higher fraction of glycolic acid. Nanoparticles formulated from polymer containing only lactide (polylactides) demonstrated lower transfection than those formulated using copolymers containing glycolide. This could again be explained based on the lower DNA release from the polylactide nanoparticles (Fig. 3a), which was probably related to the lower diffusion of DNA through the highly hydrophobic polymer matrix and also lower degradation rate of the hydrophobic polymer.

PVA is a commonly used emulsifier in the formulation of nanoparticles, mainly because the nanoparticles formed are smaller and uniform in size and are easy to redisperse in buffer or saline. It has been shown in our studies and also by others that a fraction of PVA remains associated with the nanoparticle surface even after multiple washings (13). We have previously shown that this residual PVA affects the interfacial characteristics of nanoparticles and also their cellular uptake (11). Hence, we hypothesized that the change in the interfacial properties of nanoparticles as a result of the surface-associated PVA could affect the nanoparticle-mediated gene transfection. The lower concentration of PVA (0.5% w/v) used as an emulsifier resulted in nanoparticles with lower DNA loading and larger size (Table II), but nanoparticles formulated using 2% w/v and 5% w/v PVA solution were smaller in size and had higher DNA loading than those formulated with 0.5% PVA. This could be because of the stabilizing effect of PVA on the emulsion, leading to greater entrapment of DNA into nanoparticles and smaller particle size. Because nanoparticles formulated using 0.5% w/v PVA were different in terms of DNA loading, only the nanoparticles formulated using 2% w/v and 5% w/v PVA can be used to compare the effect of nanoparticle surface-associated PVA on gene transfection. Although there was no difference in the DNA loading and release from nanoparticles formulated with 2% w/v and 5% w/v PVA, the difference in the transfection between the two formulations of nanoparticles was significant (p = 0.001, day 5 and day 7). Nanoparticles formulated with the lower concentration of PVA (2% w/v) demonstrated 12- to 20-fold higher transfection in MCF-7 than the nanoparticles formulated with higher-concentration PVA (5% w/v) (Fig. 4b). Cellular uptake studies demonstrated that nanoparticles formulated with higher concentration of PVA have reduced cellular uptake, and these results are consistent with our previously reported studies in vascular smooth muscle cells (11). Further analysis of intracellular distribution demonstrated that the nanoparticles formulated with lower concentration of PVA had a greater amount of nanoparticles in the cytoplasmic fraction than the nanoparticles formulated with a higher concentration of PVA. The difference in nanoparticle levels in the cytoplasmic fraction thus could explain the difference in the transfection levels between the two formulations of nanoparticles (2% w/v and 5% w/v PVA). Higher intracellular uptake and cytoplasmic levels of the nanoparticles formulated using 2% w/v PVA could be related to their surface charge. In our previous studies, we have shown that the surface charge reversal of the nanoparticle in the acidic pH usually found in the endolysosomes is the

mechanism of endosomal escape of nanoparticles (6). The shielding of the surface charge reversal by the presence of a higher amount of surface-associated PVA in nanoparticles (11) could affect their escape from the endolysosomal compartment to the cytoplasmic compartment.

The study also demonstrated that not only the concentration of PVA but also the type of PVA (molecular weight and degree of hydrolyzation) used in nanoparticle formulation influences gene transfection. Nanoparticles formulated using low-molecular-weight PVA demonstrated lower gene transfection compared to those formulated using higher-molecular-weight PVA despite higher DNA loading and similar DNA release from these particles. This could be related to the higher amount of residual PVA associated with the nanoparticles formulated with low-molecular-weight PVA than those formulated using higher-molecular-weight PVA (Table II). Similarly, the nanoparticles formulated using PVA of higher degree of hydrolyzation had a reduced amount of surface-associated PVA. These results are similar to those reported previously, where PLGA nanoparticles prepared by the spontaneous emulsification solvent diffusion method had a higher amount of PVA bound when PVA of lower degree of hydrolyzation was used (26). Relatively lower amounts of surface-associated PVA, higher DNA loading, and greater DNA release from the nanoparticles formulated using PVA of higher degree of hydrolyzation could explain the higher gene transfection of these nanoparticles as compared to gene transfection of the nanoparticles formulated using PVA of lower degree of hydrolyzation. Some of the differences in transfection seen with various formulations of nanoparticles prepared with different PVA could also be related to the difference in their sticking property to the cell surface through the surface-associated PVA. However, recently in rabbit conjunctival epithelial cells, we have demonstrated that about 90% of the particles associated with cells are internalized, and the remaining fraction (10%) is surface associated (unpublished results). Therefore, the influence of PVA affecting the gene expression of nanoparticles through the difference in their sticking properties to the cell surface could be marginal and appears to be mainly linked to the difference in their uptake and intracellular distribution.

Based on the influence of surface-associated PVA on gene transfection of nanoparticles, it could be speculated that the stealth nanoparticles or liposomes that are used to achieve prolonged systemic circulation would have reduced gene expression in the target cells or tissue as compared to that with nonstealth systems. In fact, Shi *et al.* (27) have demonstrated that inclusion of poly(ethylene glycol)–lipid analogues in oligonucleotide (ODN) lipoplex inhibited their internalization in Chinese hamster ovary cells by more than 70%. Furthermore, they observed that the intracellular fraction of lipoplex remained entrapped in the endolysosomal pathway, and no release of ODNs was seen.

Although we have not studied the effect of different formulation parameters on gene transfection of nanoparticles *in vivo*, it seems logical to believe that the parameters investigated in this study that influenced the DNA loading in nanoparticles, DNA release from nanoparticles, and cellular uptake of nanoparticles would also affect the gene expression of nanoparticles *in vivo*. Therefore, the conclusions drawn from the *in vitro* studies in this paper about nanoparticle formulation parameters are critical in achieving higher gene transfec-

tion *in vivo* using nanoparticles. Unlike polyplexes and lipoplexes, nanoparticles are anionic in physiologic pH and do not aggregate under the physiologic conditions or in the presence of serum. It is to be noted that all the transfection studies in this paper with nanoparticles were carried out in the presence of serum. Therefore, nanoparticles can be used *in vivo* to achieve sustained gene transfection.

CONCLUSIONS

In conclusion, various formulation factors were found to affect the nanoparticle-mediated gene transfection. Polymer characteristics such as composition and molecular weight influenced gene transfection mainly through their effect on DNA release from nanoparticles. Emulsifier characteristics influenced gene transfection through their effect on cellular uptake, endolysosomal escape, and/or DNA release. Although some of the formulation factors are interconnected, nanoparticles formulated from polymer composed of 50/50 lactide:glycolide and of high molecular weight (143 kDa) and with 2% w/v PVA (88% hydrolysis and average molecular weight of 31–50 kDa) demonstrated greater gene transfection than the other formulations investigated in this study.

REFERENCES

1. F. Liu and L. Huang. Development of non-viral vectors for systemic gene delivery. *J. Control. Rel.* **78**:259–266 (2002).
2. M. D. Brown, A. G. Schatzlein, and I. F. Uchegbu. Gene delivery with synthetic (non viral) carriers. *Int. J. Pharm.* **229**:1–21 (2001).
3. D. Lechardeur and G. L. Lukacs. Intracellular barriers to non-viral gene transfer. *Curr. Gene Ther.* **2**:183–194 (2002).
4. H. Cohen, R. J. Levy, J. Gao, I. Fishbein, V. Kousaev, S. Sosnowski, S. Slomkowski, and G. Golomb. Sustained delivery and expression of DNA encapsulated in polymeric nanoparticles. *Gene Ther.* **7**:1896–1905 (2000).
5. S. Prabha, W. Z. Zhou, J. Panyam, and V. Labhasetwar. Size-dependency of nanoparticle-mediated gene transfection: studies with fractionated nanoparticles. *Int. J. Pharm.* **244**:105–115 (2002).
6. J. Panyam, W. Z. Zhou, S. Prabha, S. K. Sahoo, and V. Labhasetwar. Rapid endo-lysosomal escape of poly(D,L-lactide-co-glycolide) nanoparticles: implications for drug and gene delivery. *FASEB J.* **16**:1217–1226 (2002).
7. K. Roy, H. Q. Mao, S. K. Huang, and K. W. Leong. Oral gene delivery with chitosan–DNA nanoparticles generates immunologic protection in a murine model of peanut allergy. *Nature Med.* **5**:387–391 (1999).
8. V. Labhasetwar, J. Bonadio, S. A. Goldstein, and R. J. Levy. Gene transfection using biodegradable nanospheres: results in tissue culture and a rat osteotomy model. *Colloid Surface B: Biointerfaces* **16**:281–290 (1999).
9. K. M. Shakesheff, C. Evora, I. I. Soriano, and R. Langer. the adsorption of poly(vinyl alcohol) to biodegradable microparticles: studied by x-ray photoelectron spectroscopy (XPS). *J. Colloid Interface Sci.* **185**:538–547 (1997).
10. M. F. Zambaux, F. Bonneaux, R. Gref, P. Maincent, E. Dellacherie, M. J. Alonso, P. Labrude, and C. Vigneron. Influence of experimental parameters on the characteristics of poly(lactic

acid) nanoparticles prepared by a double emulsion method. *J Control. Rel.* **50**:31–40 (1998).

11. S. K. Sahoo J. Panyam S. Prabha, and V. Labhasetwar. Residual polyvinyl alcohol associated with poly (D,L-lactide-co-glycolide) nanoparticles affects their physical properties and cellular uptake. *J. Control. Rel.* **82**:105–114 (2002).

12. J. Davda and V. Labhasetwar. Characterization of nanoparticle uptake by endothelial cells. *Int. J. Pharm.* **233**:51–59 (2002).

13. H. Murakami, M. Kobayashi, H. Takeuchi, and Y. Kawashima. Preparation of poly(D,L-lactide-co-glycolide) nanoparticles by modified spontaneous emulsification solvent diffusion method. *Int. J. Pharm.* **187**:143–152 (1999).

14. S. Liand and L. Huang. Nonviral gene therapy: promises and challenges. *Gene Ther.* **7**:31–34 (2000).

15. M. Nishikawa and L. Huang. Nonviral vectors in the new millennium: delivery barriers in gene transfer. *Hum. Gene Ther.* **12**:861–870 (2001).

16. V. P. Torchilin, T. S. Levchenko, R. Rammohan, N. Volodina, B. Papahadjopoulos-Sternberg, and G. G. D'Souza. Cell transfection *in vitro* and *in vivo* with nontoxic TAT peptide-liposome-DNA complexes. *Proc. Natl. Acad. Sci. USA* **100**:1972–1977 (2003).

17. M. Thomas and A. M. Klibanov. Enhancing polyethylenimine's delivery of plasmid DNA into mammalian cells. *Proc. Natl. Acad. Sci. USA* **99**:14640–14645 (2002).

18. M. L. Hedley, J. Curley, and R. Urban. Microspheres containing plasmid-encoded antigens elicit cytotoxic T-cell responses. *Nat. Med.* **4**:365–368 (1998).

19. J. Panyam and V. Labhasetwar. Biodegradable nanoparticles for drug and gene delivery to cells and tissue. *Adv. Drug Deliv. Rev.* **55**:329–347 (2003).

20. R. Wattiaux, N. Laurent, S. Wattiaux-De Coninck, and M. Jadot. Endosomes, lysosomes: their implication in gene transfer. *Adv. Drug Deliv. Rev.* **41**:201–208 (2000).

21. R. Jeyanthi, R. C. Mehta, B. C. Thanoo, and P. P. DeLuca. Effect of processing parameters on the properties of peptide-containing PLGA microspheres. *J. Microencapsul.* **14**:163–174 (1997).

22. N. B. Viswanathan, P. A. Thomas, J. K. Pandit, M. G. Kulkarni, and R. A. Mashelkar. Preparation of non-porous microspheres with high entrapment efficiency of proteins by a (water-in-oil)-in-oil emulsion technique. *J. Control. Rel.* **58**:9–20 (1999).

23. Y. Y. Hsu, T. Haoand, and M. L. Hedley. Comparison of process parameters for microencapsulation of plasmid DNA in poly(D,L-lactic-co-glycolic) acid microspheres. *J. Drug Target.* **7**:313–323 (1999).

24. R. Langer, W. D. Rhine, D. T. Hsiehand, and R. S. Bawa. Polymers for sustained release of macromolecules: Applications and control of release kinetics. In R. Baker (ed), *Controlled Release Bioactive Materials*, Academic Press, Bend, Oregon, 1980, pp. 83–98.

25. Q. R. Chenand and A. J. Mixson. Systemic gene therapy with p53 inhibits breast cancer: recent advances and therapeutic implications. *Front. Biosci.* **3**:D997–D1004 (1998).

26. H. Murakami, Y. Kawashima, T. Niwa, T. Hino, H. Takeuchiand, and M. Kobayashi. Influence of degree of hydrolyzation and polymerization of poly(vinylalcohol) on the preparation and properties of poly(D,L-lactide-co-glycolide) nanoparticle. *Int. J. Pharm.* **149**:43–49 (1997).

27. F. Shi, L. Wasungu, A. Nomden, M. C. Stuart, E. Polushkin, J. B. Engbertsand, and D. Hoekstra. Interference of poly(ethylene glycol)-lipid analogues with cationic-lipid-mediated delivery of oligonucleotides; role of lipid exchangeability and non-lamellar transitions. *Biochem. J.* **366**:333–341 (2002).

Fluorescence and electron microscopy probes for cellular and tissue uptake of poly(D,L-lactide-co-glycolide) nanoparticles

Jayanth Panyam[a], Sanjeeb K. Sahoo[a], Swayam Prabha[a], Tom Bargar[b], Vinod Labhasetwar[a,c,*]

[a] Department of Pharmaceutical Sciences, University of Nebraska Medical Center, Omaha, NE 68198, USA
[b] Department of Genetics, Cell Biology and Anatomy, University of Nebraska Medical Center, Omaha, NE 68198, USA
[c] Department of Biochemistry and Molecular Biology, University of Nebraska Medical Center, Omaha, NE 68198, USA

Abstract

Nanoparticles formulated from poly(D,L-lactide-co-glycolide) (PLGA) and poly(lactide) (PLA) are being extensively investigated for different therapeutic applications such as for sustained drug, vaccine, and gene delivery. For many of these applications, it is necessary to study the intracellular distribution as well as the tissue uptake of nanoparticles to optimize the efficacy of the encapsulated therapeutic agent. Fluorescence and electron microscopic techniques are usually used for the above purposes. Colloidal gold particles and fluorescent polystyrene, which are generally used as model particles for electron and fluorescence microscopy, respectively, may not be suitable alternatives to PLGA/PLA nanoparticles for these studies mainly because of the differences in their physical properties and also because they do not contain any therapeutic agent. The aim of the present study was to develop and characterize PLGA nanoparticle formulations that would be suitable for confocal/fluorescence and transmission electron microscopic (TEM) studies. Towards this objective, PLGA nanoparticles containing 6-coumarin as a fluorescent marker and osmium tetroxide as an electron microscopic marker with bovine serum albumin (BSA) as a model protein were formulated. Different physical properties of marker-loaded nanoparticles such as particle size, zeta potential, residual PVA content and protein-loading were compared with those of unloaded nanoparticles and were found to be not significantly different. Furthermore, marker-loaded nanoparticle formulations were non-toxic to the cells as unloaded nanoparticles. Nanoparticles loaded with 6-coumarin were found to be useful for studying intracellular nanoparticle uptake and distribution using confocal microscopy while osmium tetroxide-loaded nanoparticles were found to be useful for studying nanoparticle uptake and distribution in cells and tissue using TEM. It was concluded that 6-coumarin and osmium tetroxide could serve as useful fluorescence and electron microscopy probes, respectively, for incorporation into nanoparticles to study their cellular and tissue distribution.
© 2003 Elsevier B.V. All rights reserved.

Keywords: Drug delivery; Biodegradable polymers; Transmission electron microscopy; Confocal microscopy

1. Introduction

Nanoparticles formulated from the biocompatible and biodegradable polymers, poly(D,L-lactide-co-glycolide) (PLGA) and poly(lactide) (PLA), are being extensively investigated for different therapeutic applications such as for sustained drug, vaccine, and

* Corresponding author. Tel.: +1-402-559-9021;
fax: +1-402-559-9543.
E-mail address: vlabhase@unmc.edu (V. Labhasetwar).

gene delivery (Moghimi et al., 2001; Panyam and Labhasetwar, 2003a). For a number of these applications, it is important to study the kinetics of cellular and tissue uptake, intracellular distribution and retention, and in vivo biodistribution of nanoparticles (Panyam and Labhasetwar, 2003b). For example, it might be necessary to study the efficiency of nanoparticle localization in a particular cell population, organ or specific tissue following their local or systemic administration to optimize drug therapy (Lamprecht et al., 2001; Panyam et al., 2002b). Similarly, it is necessary to study the effect of various nanoparticle formulation parameters and their physical properties (e.g. surface charge, particle size) on cellular uptake of nanoparticles and their distribution in various cellular compartments (e.g. endo-lysosomes, cytoplasm, nucleus, etc.). Understanding of the intracellular and tissue distribution of nanoparticles is also useful to elucidate the mechanism of enhanced therapeutic efficacy of nanoparticle-encapsulated therapeutic agents (Demoy et al., 1999; Prabha et al., 2002; Sahoo et al., 2002; Desai et al., 1997).

For many of these applications, fluorescent polystyrene nanoparticles are used as a model for PLGA/PLA nanoparticles so that nanoparticle uptake and distribution can be visualized by either confocal or fluorescence microscopy or quantified by analyzing the extracted fluorescent dye (Zauner et al., 2001). Similarly, colloidal gold particles are used as a model for studying nanoparticle uptake and distribution by transmission electron microscopy (TEM) because of their electron dense nature (McIntosh et al., 2002). However, physical properties of these model nanoparticles including hydrophobicity, surface charge, particle size distribution, density and protein adsorption could be different from that of PLGA/PLA nanoparticles. For example, polystyrene nanoparticles are more hydrophobic than PLGA nanoparticles (Norris et al., 1999). Although polystyrene nanoparticles are available with different surface functional groups on the surface (e.g. carboxylated or amine modified), typical non-functionalized polystyrene nanoparticles have a markedly more negative zeta potential than PLGA nanoparticles due to the presence of small number of sulfate groups on the surface (Panyam et al., 2002b). Also, PLGA nanoparticles are cationic in acidic pH and anionic in neutral and alkaline pH whereas polystyrene nanoparticles are anionic in all pH values

(Panyam et al., 2002b). In our recent studies, cationization of PLGA nanoparticles in the acidic pH of endo-lysosomal compartment has been demonstrated as the mechanism for their escape into cytoplasmic compartment, signifying the role of surface charge on intracellular distribution of nanoparticles (Panyam et al., 2002b). In addition, PLGA/PLA nanoparticles are typically prepared using an emulsifier (e.g. polyvinyl alcohol, PVA). Recently, we have shown that residual PVA associated with PLGA nanoparticles significantly affects their interfacial as well as cellular uptake properties (Sahoo et al., 2002). The results of the above study thus suggest the importance of interfacial properties of nanoparticles towards their interaction with cells. Further, no therapeutic agent can be encapsulated in the above model nanoparticles, which could also affect the surface properties of nanoparticles. Hence, the results obtained with polystyrene or gold nanoparticles might not truly represent what would be seen with PLGA/PLA nanoparticles.

To overcome this problem, studies by other investigators have attempted to use radiolabeled-polymer for formulating nanoparticles and then quantify the radioactivity to follow the uptake and distribution (Le Ray et al., 1994). However, the limitation of this approach is that the uptake and distribution of these nanoparticles in different intracellular compartments or uptake by a particular cell population in a tissue sample cannot be followed by microscopic techniques. Furthermore, for studies using TEM, cell and tissue contain many vesicles, which look like nanoparticles, and oftentimes, it is difficult to distinguish them from nanoparticles, as PLGA or PLA are not electron dense polymers.

The aim of the present study was to identify suitable probes that can be incorporated into nanoparticles along with a therapeutic agent that would be suitable for confocal/fluorescence microscopy and TEM studies. Bovine serum albumin (BSA) was used as a model protein for encapsulation in nanoparticles. We have characterized 6-coumarin, a lipophilic fluorescent dye, incorporated in nanoparticles as a marker for confocal microscopy to study nanoparticle uptake in cells. Similarly, we have determined the suitability of osmium tetroxide, an electron dense agent, incorporated in nanoparticles as a marker to study nanoparticle uptake in cells and tissues using TEM.

2. Materials and methods

2.1. Materials

BSA (Fraction V) and PVA (average molecular weight, 30,000–70,000) were purchased from Sigma (St. Louis, MO). LysoTracker® Red was purchased from Molecular Probes (Eugene, OR). 6-Coumarin was purchased from Polysciences (Warrington, PA). PLGA (50:50 lactide–glycolide ratio, 143,000 Da) was purchased from Birmingham Polymers (Birmingham, AL). All the reagents used for TEM were from Electron Microscopy Services (Ft. Washington, PA).

2.2. Methods

2.2.1. Nanoparticle formulation

Nanoparticles containing BSA and 6-coumarin were formulated using a double emulsion-solvent evaporation technique as described previously (Davda and Labhasetwar, 2002). An aqueous solution of BSA (60 mg/ml, 1 ml) was emulsified in a PLGA solution (180 mg in 6 ml chloroform) containing 6-coumarin (100 μg) using a probe sonicator (55 W for 2 min) (Sonicator® XL, Misonix, NY). The water-in-oil emulsion formed was further emulsified into 50 ml of 2.5% w/v aqueous solution of PVA by sonication (55 W for 5 min) to form a multiple water-in-oil-in-water emulsion. The multiple emulsion was stirred for ∼18 h at room temperature followed by for 1 h in a desiccator under vacuum to remove the residual chloroform. Nanoparticles were recovered by ultracentrifugation (35,000 rpm for 20 min at 4 °C, Optima™ LE-80K, Beckman, Palo Alta, CA), washed two times with distilled water to remove PVA, unentrapped BSA and 6-coumarin, and then lyophilized (−80 °C and <10 μm mercury pressure, Sentry™, Virtis, Gardiner, NY) for 48 h to obtain a dry powder. Nanoparticles containing osmium tetroxide were formulated similarly, except, instead of 6-coumarin, 10 mg osmium tetroxide was added to the polymer solution prior to emulsification. Dry lyophilized nanoparticle samples were stored in a dessicator at 4 °C and were reconstituted in a suitable medium (buffer or cell culture medium) prior to an experiment.

2.2.2. Nanoparticle characterization

2.2.2.1. Particle size and surface charge (zeta potential).
Particle size and size distribution were determined by photon correlation spectroscopy (PCS) using quasi-elastic light scattering equipment (ZetaPlus™ equipped with particle sizing mode, Brookhaven Instrument Crop., Holtsville, NY). A dilute suspension (100 μg/ml) of nanoparticles was prepared in double distilled water and sonicated on an ice bath for 30 s. The sample was subjected to particle size analysis. Zeta potential of nanoparticles in 0.001 M HEPES buffer, pH 7.4 (0.5 mg/ml) was determined using ZetaPlus™ in the zeta potential analysis mode.

2.2.2.2. Protein loading.
Amount of BSA encapsulated in nanoparticles was determined by analyzing the protein content in the washings from the nanoparticle formulation step. Protein content was measured using BCA protein assay kit (Pierce, Rockford, IL). Protein loading in nanoparticles was calculated by subtracting the amount of protein present in the washings from the total protein added.

2.2.2.3. Residual PVA content.
Residual amount of PVA associated with nanoparticles was determined by a colorimetric method (Sahoo et al., 2002). In brief, 2 mg of lyophilized nanoparticle sample was treated with 2 ml of 0.5 M NaOH for 15 min at 60 °C. Samples were neutralized with 900 μl of 1N HCl and the volume was adjusted to 5 ml with distilled water. To each sample, 3 ml of a 0.65 M solution of boric acid, 0.5 ml of I_2/KI (0.05/0.15 M) solution, and 1.5 ml of distilled water were added. Finally, the visible spectra absorbance of the samples was measured at 690 nm (UV-1601PC UV-Vis Spectrophotometer, Shimadzu Scientific Instruments, Columbia, MD) after 15 min incubation. A standard plot of PVA was prepared under identical conditions.

2.2.2.4. In vitro release of 6-coumarin.
To determine the amount of 6-coumarin released from nanoparticles under different pH conditions, nanoparticles were incubated with 0.1 M HEPES buffer of pH 4 and 7.4. Buffers of pH 4 and 7.4 were selected for the in vitro release studies to represent the pH present in the endo-lysosomal compartment and physiologic pH, respectively. About 1 mg of 6-coumarin-loaded nanoparticles was dispersed in 0.5 ml of HEPES

buffer, which was then placed inside a Spectra/Por® CE cellulose ester DispoDialyzer dialysis bags (300,000 Da molecular weight cut-off, Pierce). Each dialysis bag was then placed in 9.5 ml of HEPES buffer contained in 15 ml centrifuge tubes (Becton Dickinson). The whole set up was then incubated at 37 °C and shaken at 100 rpm (Environ® orbital shaker, Lab Line, Melrose Park, IL). Samples (1.0 ml) were taken from outside the dialysis bag and replaced with fresh buffer. Samples were lyophilized (−80 °C and <10 μm mercury pressure, Sentry™, Virtis) and then reconstituted in 1 ml methanol. Amount of 6-coumarin in the release samples was analyzed by our previously reported HPLC method (Davda and Labhasetwar, 2002). Care was taken to protect the samples from light throughout the experimental procedure.

2.2.3. Biocompatibility studies

Human vascular smooth muscle cells (abbreviated as VSMCs, Cascade Biologics, Portland, OR) cultured in Medium 231 with added smooth muscle growth supplement (Cascade Biologics) and 100 μg/ml penicillin G and 100 μg/ml streptomycin (Gibco BRL, Grand Island, NY), were used for all the cell culture studies. The cells were seeded at 5000 cells per well/0.1 ml (50% confluency) in a 96-well plate and allowed to attach overnight. Marker-loaded nanoparticles were added at different doses in 0.1 ml of the medium and incubated for 2 days. Untreated cells (plain medium) were used as a control. Polyethylenimine (25 kDa, Aldrich, Milwaukee, WI) was used a positive control for the assay. At the end of the incubation period, cells were washed twice with phosphate buffered saline (PBS, pH 7.4) to remove nanoparticles and 0.1 ml of fresh medium was added to each well. The viability of the cells was determined using MTS assay (CellTiter 96 AQ$_{ueous}$, Promega, Madison, WI). The MTS reagent (20 μl) was added to each well, incubated for 150 min and the absorbance was measured at 490 nm using a microplate reader (BT 2000 Microkinetics Reader, BioTek Instruments, Inc., Winooski, VT).

2.2.4. Confocal microscopic studies

VSMCs were plated in Bioptech® plates (Bioptechs, Butler, PA) at 50,000 cells per plate (50% confluency) in 1 ml of growth medium and allowed to attach for 24 h. Cells were then incubated with 6-coumarin-loaded nanoparticle suspension (100 μg/ml) in growth medium for 60 min. Cells were then washed twice with PBS and visualized with HEPES buffer (pH 8) using a Zeiss Confocal LSM410 microscope equipped with Argon–Krypton laser (Carl Zeiss Microimaging, Inc., Thornwood, NY).

2.2.5. TEM studies

TEM of control nanoparticles was performed by negative staining with uranyl acetate. A drop of nanoparticle suspension (1 mg/ml) was placed on Formvar®-coated copper grids (150 mesh, Ted Pella Inc., Redding, CA) and allowed to equilibrate. Excess liquid was removed with a filter paper and a drop of 2% w/v uranyl acetate was added to the grid. After 3 min of incubation at room temperature, excess liquid was removed and the grid was air-dried. The dried grid containing the nanoparticles was visualized using a Philips 201® transmission electron microscope (Philips/FEI Inc., Briarcliff Manor, NY). Osmium tetroxide-loaded nanoparticles were visualized without the negative staining.

For cell uptake studies, VSMCs were plated 24 h prior to the experiment in 100-mm tissue culture dishes (Becton Dickinson) at 500,000 cells per dish in 10 ml of growth medium. Cells were incubated with osmium tetroxide-loaded nanoparticle suspension (100 μg/ml) and were washed twice with PBS at 1 h post incubation. Cells were harvested by trypsinization and then fixed in a 2.5% glutaraldehyde solution in PBS for 1 h and then post-fixed in 1% osmium tetroxide in PBS for 1 h. Fixed cells were washed with Sörenson's PBS and dehydrated three times sequentially in a graded series of ethanol solutions (50, 70, 90, 95, and 100%); they were then soaked overnight in a 1:1 ratio of 100% ethyl alcohol and Unicryl® embedding resin (Ted Pella Inc.), and then in fresh Unicryl® resin for 4–5 h. The resin-embedded cells were placed in BEEM capsules (EMS), and the capsules were placed in a Pelco UV-2 Cryo Chamber (Ted Pella Inc.) at 4 °C for 48 h for polymerization of the resin by UV radiation. The polymerized blocks were sectioned and the sections (80–100 nm thick) were placed on Formvar®-coated copper grids (150 mesh, Ted Pella Inc.), stained with an aqueous solution of 2% uranyl acetate for 15 min, washed briefly in water, stained with Reynold's lead citrate for 7 min, and then finally washed in water prior to visualization under a Philips 210® microscope (Philips/FEI Inc.).

Table 1
Physical characterization of marker-loaded PLGA nanoparticles

Nanoparticles with or without markers	Particle size ± S.E.M. (nm)[a] ($n = 5$)	Zeta potential ± S.E.M. (mV)[b] ($n = 5$)	Protein loading (% w/w)	Encapsulation efficiency (%) of protein	Percent of residual PVA content (w/w)	Marker loading (% w/w)[c]
6-Coumarin	263 ± 6	−12.6 ± 1.4	22.3	66	4.6 ± 0.2	0.05
Osmium tetroxide	297 ± 12	−10.6 ± 1.4	19.2	57	5.5 ± 0.4	nd
Without marker	267 ± 10	−7.9 ± 1.8	17.8	53	4.2 ± 0.4	–

[a] Mean hydrodynamic diameter measured by photon correlation spectroscopy.
[b] Measured in 0.001 M HEPES buffer, pH 7.4.
[c] nd: not determined.

For tissue distribution studies, male athymic nude mice (2–3 weeks age, 20–30 g weight, Charles River Laboratories, Wilmington, MA) were used. Animals were maintained in a pathogen-free environment and handled according to the *Guide for the Care and Use of Laboratory Animals* published by the U.S. National Institutes of Health (NIH Publication No. 85-23, revised 1996) and the ethical guidelines of the University of Nebraska Medical Center Institutional Animal Care and Use Committee.

Osmium tetroxide-loaded nanoparticles were suspended in Hank's balanced salt solution (1 mg/ml) and injected intramuscularly into the left thigh of the animal (200 μl per animal). Right thigh muscles were injected with vehicle and were used as controls. One hour following the injection, mice were euthanized and the muscle tissue samples were collected, cut into ~1 mm³ pieces and then fixed in 2.5% glutaraldehyde solution in PBS. Post-fixation, embedding, sectioning, and staining procedures were performed similar to that described for cell culture samples.

3. Results and discussion

3.1. Nanoparticle characterization

Table 1 describes the physical characterization of different nanoparticle formulations. All the nanoparticle formulations had a mean diameter in the size range
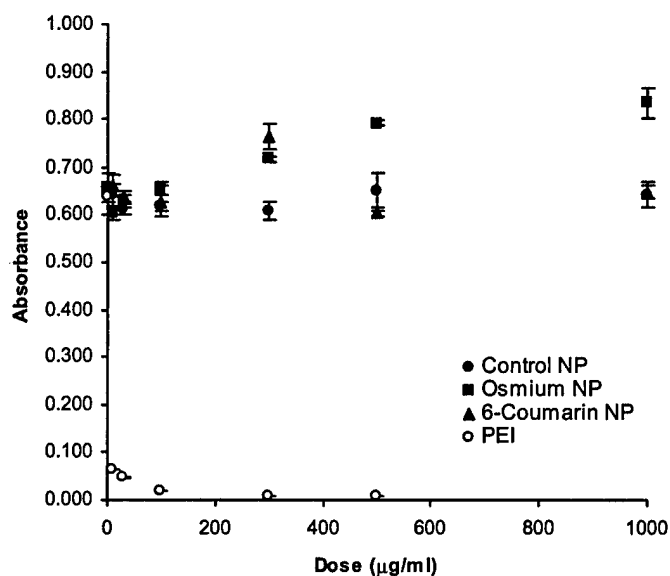

Fig. 1. Biocompatibility of marker-loaded nanoparticles. VSMCs were incubated with different doses of nanoparticles and the viability of the cells was determined by MTS assay. Polyethylenimine was used as a positive control.

of 250–300 nm with log normal size distribution as measured by dynamic light scattering and had a zeta potential in the range of −7.9 to −12.6 mV at pH 7.4. The percent of residual PVA was in the range of 4.2–5.5% w/w. All the nanoparticle formulations had similar protein loading, the range being 18–22% w/w.

Previous studies have shown that particle size is an important property that affects t he intracellular uptake of nano- and microparticles, with smaller size particles, in general, having higher uptake (Desai et al., 1997). Particle size could also affect the efficacy of nanoparticle-encapsulated therapeutic agents. We have shown that smaller size nanoparticles have higher transfectivity compared to larger size nanoparticles in vitro (Prabha et al., 2002). Similarly, we have shown that zeta potential of nanoparticles plays an important role in affecting the intracellular trafficking

of nanoparticles. Nanoparticles that show a reversal in their zeta potential (from anionic to cationic) in acidic pH (e.g. PLGA nanoparticles) can escape the degradative endo-lysosomal compartment into the cytosol, whereas nanoparticles that remain anionic at all pH values (e.g. polystyrene nanoparticles) do not exhibit endo-lysosomal escape (Panyam et al., 2002b). Further, we have shown that residual PVA content of nanoparticles affects the cellular uptake properties of nanoparticles, with nanoparticles containing lower amounts of residual PVA demonstrating higher uptake (Sahoo et al., 2002). Thus, the above physical characteristics of nanoparticles are important in determining their intracellular uptake and trafficking of nanoparticles. As seen from Table 1, nanoparticles containing the markers had similar physical characteristics as that of nanoparticles without any marker.
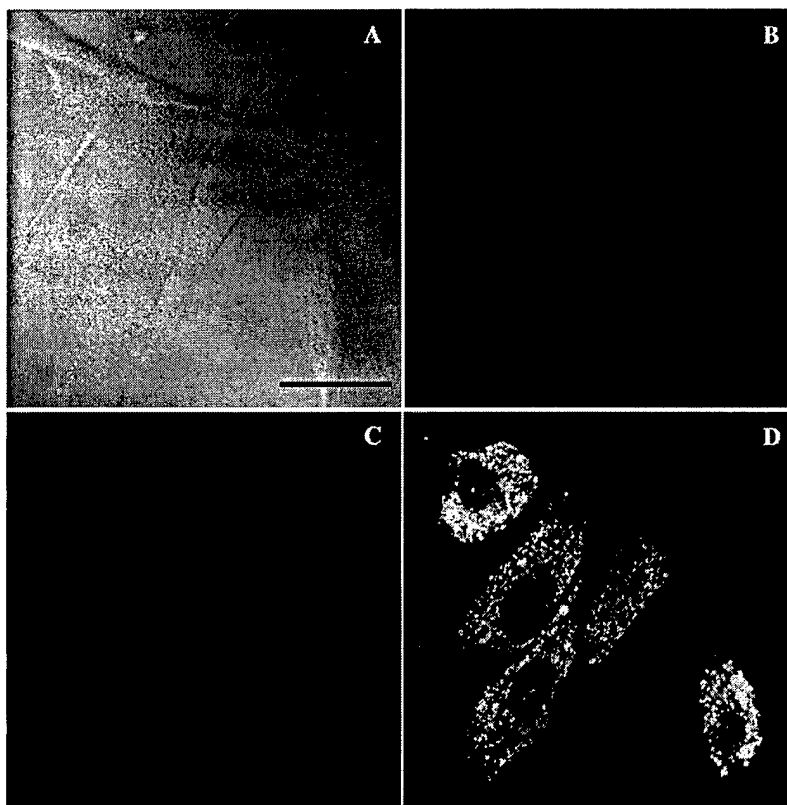

Fig. 2. Confocal microscopic images demonstrating the intracellular distribution of 6-coumarin-loaded nanoparticles in VSMCs. (A) Differential interference contrast image showing the outline of the cells. (B) Cells stained with LysoTracker® Red and visualized using RITC filter. (C) Uptake of green fluorescent 6-coumarin-loaded nanoparticles in VSMCs visualized using FITC filter. (D) Overlay of (B) and (C) showing the co-localization of nanoparticles with endo-lysosomes. Bar represents 25 μm.

One concern in using osmium tetroxide and 6-coumarin as markers for nanoparticles is their biocompatibility. Osmium tetroxide is known to be toxic and is a potent irritant. Nanoparticles should therefore not release the marker in significant amounts during the time period of the study, which could result in acute toxicity. Hence, we tested the biocompatibility of marker-loaded nanoparticles in cell culture. As seen from Fig. 1, there was no acute toxicity associated with either 6-coumarin- or osmium tetroxide-loaded nanoparticles compared to either control nanoparticle-treated or untreated (plain medium) cells. Polyethylenimine, a commonly used gene transfection reagent (Boussif et al., 1995), showed significant cytotoxicity in the concentration range tested (~80% toxicity at 2 μg/ml dose).

3.2. 6-Coumarin-loaded nanoparticles for fluorescence microscopy

Nanoparticles loaded with 6-coumarin were characterized for the leaching of dye in two different pH buffers. We have previously shown that under physiological conditions such as in pH 7.4 buffer or in the presence of lipids (to simulate membrane lipids),

less than 0.5% of the dye is released, suggesting the suitability of 6-coumarin as a marker for nanoparticles (Desai et al., 1996; Davda and Labhasetwar, 2002). However, recent studies have shown that nanoparticles, following their intracellular uptake, are trafficked through an acidic endo-lysosomal compartment (pH 4–5) (Panyam et al., 2002b). Hence, it is pertinent to test the release of the dye in acidic pH to ensure that green fluorescence seen inside the cells in confocal microscopy (Fig. 2) is not due to the dye released in acidic pH. About 0.10% of the encapsulated dye was released in pH 4 compared to about 0.45% release observed in pH 7.4 in 48 h (Fig. 3), suggesting that dye is not released in acidic pH present in endo-lysosomes. Thus, 6-coumarin has the advantage over other dyes which show pH-dependent solubility. For example, rhodamine forms a water-soluble salt in acidic pH (ref. Merck Index, 12th edition) and hence, the dye could be released from nanoparticles in the endo-lysosomes, which could result in inaccurate intracellular distribution pattern.

From the above results, it can be seen that 6-coumarin could be a useful probe for fluorescence/confocal microscopic studies. The other advantages
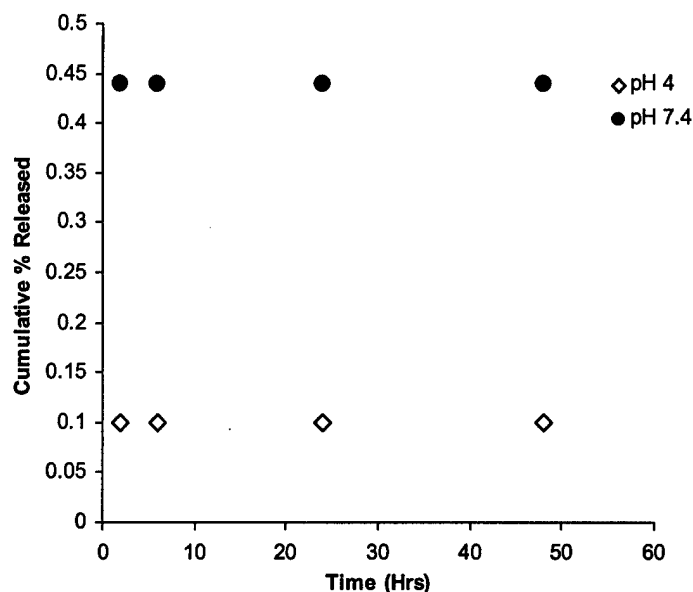

Fig. 3. In vitro release of 6-coumarin from nanoparticles in HEPES buffer (0.15 M) of pH 4 and 7.4. Standard deviations were less than 1% in all the cases.

of 6-coumarin include the requirement of low dye loading in nanoparticles due to its high fluorescence activity. About 0.05% w/w dye loading in the particles results in brightly fluorescent nanoparticles (Fig. 2). The uptake of these nanoparticles can be easily visualized by confocal microscopy. Most cells that were tested (VSMCs, vascular endothelial cells, COS-7 and HEK-293) do not have background fluorescence in the fluorescence emission range of 6-coumarin. Another advantage of 6-coumarin is the possibility of its quantitation by HPLC. We have previously reported a sensitive HPLC method to quantitate 6-coumarin in both cell lysates and in tissue samples (Panyam et al., 2002a; Davda and Labhasetwar, 2002). The assay is sensitive, with detection limit of 5 ng of nanoparticles. Also, due to its high lipid solubility, dye can be extracted from cell lysates and tissue samples using organic solvents such as methanol or ethyl acetate with extraction efficiency close to 95%.

6-Coumarin-labeled nanoparticles can be used to study the intracellular distribution by using co-localization techniques. Using an organelle-specific dye with contrasting fluorescence, it is possible to study the co-localization of nanoparticles in the particular organelle. For example, using LysoTracker® Red, a pH sensitive dye that emits red fluorescence in acidic pH, and 6-coumarin-loaded nanoparticles, it was possible to determine the presence of nanoparticles in the acidic endo-lysosomal vesicles. Presence of green fluorescent nanoparticles in red fluorescent vesicles shows up as yellow fluorescence in the over-
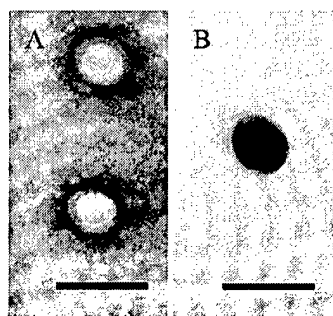

Fig. 4. TEM images of (A) control (blank) nanoparticles and (B) osmium tetroxide-loaded nanoparticles. Control nanoparticles were visualized following negative staining with 2% w/v uranyl acetate. Bar represents 250 nm (31,000× magnification).
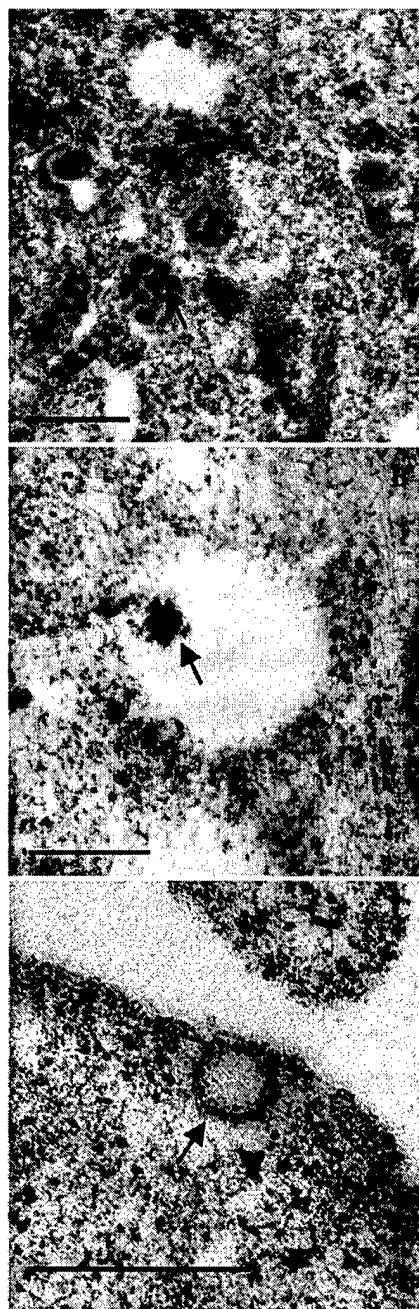

Fig. 5. TEM images showing (A) nanoparticles (indicated by arrow) present in the cytoplasm (16,900×), (B) a nanoparticle (indicated by arrow) interacting with vesicular membrane (21,000×), and (C) control VSMCs (untreated cells) with nanoparticle-like vesicles of approximately 100 nm (indicated by arrow) (38,000×). Bars represent 500 nm.

lay (Fig. 2). The same approach can be used to study the co-localization of nanoparticles in other organelles such as the nucleus or mitochondria using specific fluorescent dyes.

6-Coumarin-loaded nanoparticles can also be used for acute in vivo pharmacokinetics and tissue distribution studies. These nanoparticles were used in our previous studies for comparing the efficiency of two infusion catheters in localizing nanoparticles in balloon-injured artery (Panyam et al., 2002a). Also nanoparticle distribution in arterial section was determined using fluorescence microscopy. Thus, using 6-coumarin as a marker, the differences in the nanoparticle distribution in different tissue can be visualized as well as their levels quantitated.

3.3. Osmium tetroxide-loaded nanoparticles for electron microscopy

Previous approaches to study the tissue or intracellular distribution of nanoparticles by electron microscopy have mostly used gold or gold-labeled particles (McIntosh et al., 2002) since gold is electron-dense and gold particles are available in pre-defined sizes. However, being metallic in nature, gold particles would have widely different properties compared to that of polymer particles used in drug delivery. Hence, osmium tetroxide was investigated as an electron microscopy marker for PLGA nanoparticles. Osmium tetroxide is an electron dense agent that has been previously used for post-fixation and
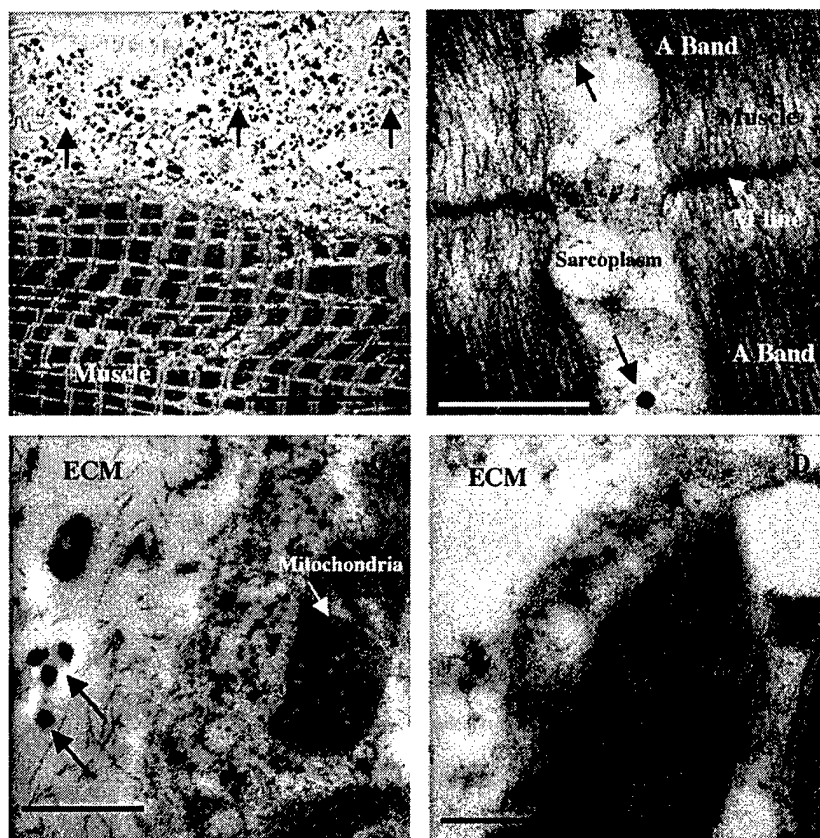

Fig. 6. (A) Low magnification TEM image (1600×) of muscle tissue showing nanoparticles (indicated by arrows) mainly in ECM and some in the muscle fibers. (B) Higher magnification (31,000×) image showing the presence of nanoparticles in the sarcoplasm of the muscle cell (indicated by black arrow). Dark band (A band) and M line can be seen in the muscle fibril. (C) Nanoparticles (black arrow) can be easily distinguished from other intracellular structures like mitochondria (striated structure, white arrow) at high magnifications (31,000×). (D) TEM image of control tissue from the uninjected thigh muscle (31,000×). In (A) bar represents 10 μm whereas in (B), (C) and (D), bar represents 500 nm.

staining cells for transmission electron microscopy. It has high affinity for lipids and hence has been used for staining lipids in cells and tissue. Because of its solubility in organic solvents, osmium tetroxide can be easily dissolved along with the polymer solution prior to emulsification.

Fig. 4 shows the transmission electron microscopic images of control nanoparticles and osmium tetroxide-loaded nanoparticles. The control particles required negative staining with uranyl acetate to be visible under an electron beam while osmium tetroxide particles are visible without any staining due to the electron dense nature of osmium tetroxide. It was possible to clearly distinguish the nanoparticles within the cellular compartments because of their distinct dark color (Fig. 5A and B). PLGA nanoparticles without any marker could not be used to study the intracellular uptake and localization of nanoparticles since it was difficult to distinguish between intracellular vesicles from nanoparticles (Fig. 5C).

In order to determine the suitability of osmium tetroxide-loaded nanoparticles for studying tissue distribution using TEM, these particles were injected into mouse thigh muscle. Following intramuscular administration, a major fraction of the nanoparticles was found in the extracellular matrix of the muscle tissue (Fig. 6A). It is possible that the negatively charged nanoparticles are attracted to cationic molecules such as proteoglycans in the ECM. However, it is expected that this phenomenon would be similar for all the PLGA nanoparticle formulations since all of them have similar negative zeta potential values (Table 1). Some nanoparticles were taken up by the muscle cells and were found in the sarcoplasm (Fig. 6B). Nanoparticles could be identified as dark spherical structures, about 100–200 nm in size. At lower magnification, it was difficult to distinguish nanoparticles from mitochondria since they are also dark colored structures. However, at higher magnification, mitochondria could be easily distinguished due to their shape, size and the presence of distinct striations (Fig. 6C). Control tissue did not show black spherical structures (Fig. 6D).

4. Limitations

While these microscopy markers have been shown to be useful in acute studies, their usefulness in chronic studies is not yet determined. Although <1% of 6-coumarin leaches out from nanoparticles in aqueous medium over a 48 h period, the in vivo or intracellular fate of the dye over a longer time period is yet to be studied. Similarly, osmium tetroxide-loaded particles did not demonstrate any toxicity over a period of 2 days, however, their long-term biocompatibility is not known.

5. Conclusions

We have characterized nanoparticles containing 6-coumarin and osmium tetroxide as fluorescent and transmission electron microscopic probes, respectively. The formulation characteristics of nanoparticles containing the probes were similar to that of unloaded nanoparticles. Encapsulation of the markers did not affect the biocompatibility of nanoparticles. It can be concluded that these nanoparticles could serve as useful probes for studying nanoparticle uptake, retention and distribution in vivo and in vitro.

References

Boussif, O., Lezoualc'h, F., Zanta, M.A., Mergny, M.D., Scherman, D., Demeneix, B., Behr, J.P., 1995. A versatile vector for gene and oligonucleotide transfer into cells in culture and in vivo:

polyethylenimine. Proc. Natl. Acad. Sci. U.S.A. 92, 7297–7301.

Davda, J., Labhasetwar, V., 2002. Characterization of nanoparticle uptake by endothelial cells. Int. J. Pharm. 233, 51–59.

Demoy, M., Andreux, J.P., Weingarten, C., Gouritin, B., Guilloux, V., Couvreur, P., 1999. Spleen capture of nanoparticles: influence of animal species and surface characteristics. Pharm. Res. 16, 37–41.

Desai, M.P., Labhasetwar, V., Amidon, G.L., Levy, R.J., 1996. Gastrointestinal uptake of biodegradable microparticles: effect of particle size. Pharm. Res. 13, 1838–1845.

Desai, M.P., Labhasetwar, V., Walter, E., Levy, R.J., Amidon, G.L., 1997. The mechanism of uptake of biodegradable microparticles in Caco-2 cells is size dependent. Pharm. Res. 14, 1568–1573.

Lamprecht, A., Schafer, U., Lehr, C.M., 2001. Size-dependent bioadhesion of micro- and nanoparticulate carriers to the inflamed colonic mucosa. Pharm. Res. 18, 788–793.

Le Ray, A.M., Vert, M., Gautier, J.C., Benoit, J.P., 1994. End-chain radiolabeling and in vitro stability studies of radiolabeled poly(hydroxy acid) nanoparticles. J. Pharm. Sci. 83, 845–851.

McIntosh, D.P., Tan, X.Y., Oh, P., Schnitzer, J.E., 2002. Targeting endothelium and its dynamic caveolae for tissue-specific transcytosis in vivo: a pathway to overcome cell barriers to drug and gene delivery. Proc. Natl. Acad. Sci. U.S.A. 99, 1996–2001.

Moghimi, S.M., Hunter, A.C., Murray, J.C., 2001. Long-circulating and target specific nanoparticles: theory to practice. Pharmacol. Rev. 53, 283–318.

Norris, D.A., Puri, N., Labib, M.E., Sinko, P.J., 1999. Determining the absolute surface hydrophobicity of microparticulates using thin layer wicking. J. Control Release 59, 173–185.

Panyam, J., Labhasetwar, V., 2003a. Biodegradable nanoparticles for drug and gene delivery to cells and tissue. Adv. Drug Deliv. Rev. 55, 329–347.

Panyam, J., Labhasetwar, V., 2003b. Dynamics of endocytosis and exocytosis of poly(D,L-lactide-co-glycolide) nanoparticles in vascular smooth muscle cells. Pharm. Res. 20, 210–218.

Panyam, J., Lof, J., O'Leary, E., Labhasetwar, V., 2002a. Efficiency of Dispatch® and Infiltrator® cardiac infusion catheters in arterial localization of nanoparticles in a porcine coronary model of restenosis. J. Drug Target 10, 515–523.

Panyam, J., Zhou, W.Z., Prabha, S., Sahoo, S.K., Labhasetwar, V., 2002b. Rapid endo-lysosomal escape of poly(D,L-lactide-co-glycolide) nanoparticles: implications for drug and gene delivery. FASEB J. 16, 1217–1226.

Prabha, S., Zhou, W.Z., Panyam, J., Labhasetwar, V., 2002. Size-dependency of nanoparticle-mediated gene transfection: studies with fractionated nanoparticles. Int. J. Pharm. 244, 105–115.

Sahoo, S.K., Panyam, J., Prabha, S., Labhasetwar, V., 2002. Residual polyvinyl alcohol associated with poly(D,L-lactide-co-glycolide) nanoparticles affects their physical properties and cellular uptake. J. Control Release 82, 105–114.

Zauner, W., Farrow, N.A., Haines, A.M., 2001. In vitro uptake of polystyrene microspheres: effect of particle size cell line and cell density. J. Control Release 71, 39–51.